arXiv:1502.01947v5 [astro-ph.GA] 19 Apr 2016

The Cusp/Core problem: supernovae feedback versus the baryonic clumps and dynamical friction model

A. Del Popolo[1,2,3] • **F. Pace**[4]

Abstract In the present paper, we compare the predictions of two well known mechanisms considered able to solve the cusp/core problem (a. supernova feedback; b. baryonic clumps-DM interaction) by comparing their theoretical predictions to recent observations of the inner slopes of galaxies with masses ranging from dSphs to normal spirals. We compare the α-$V_{\rm rot}$ and the α-M_* relationships, predicted by the two models with high resolution data coming from (Adams et al. 2014; Simon et al. 2005), LITTLE THINGS (Oh et al. 2015), THINGS dwarves (Oh et al. 2011a,b), THINGS spirals (Oh et al. 2015), Sculptor, Fornax and the Milky Way. The comparison of the theoretical predictions with the complete set of data shows that the two models perform similarly, while when we restrict the analysis to a smaller subsample of higher quality, we show that the method presented in this paper (baryonic clumps-DM interaction) performs better than the one based on supernova feedback. We also show that, contrarily to the first model prediction, dSphs of small mass could have cored profiles. This means that observations of cored inner profiles in dSphs having a stellar mass $< 10^6 M_\odot$ not necessarily imply problems for the ΛCDM model.

Keywords cosmology: theory - large scale structure of universe - galaxies:formation

A. Del Popolo

F. Pace

[1]Dipartimento di Fisica e Astronomia, Università di Catania, Viale Andrea Doria 6, 95125 Catania, Italy

[2]INFN sezione di Catania, Via S. Sofia 64, I-95123 Catania, Italy

[3]International Institute of Physics, Universidade Federal do Rio Grande do Norte, 59012-970 Natal, Brazil

[4]Jodrell Bank Centre for Astrophysics, School of Physics and Astronomy, The University of Manchester, Manchester, M13 9PL, U.K.

1 Introduction

The ΛCDM model is a highly successful paradigm at large scales (Del Popolo 2007; Komatsu et al. 2011; Del Popolo 2013; Hinshaw et al. 2013; Del Popolo 2014a; Planck Collaboration XVI 2014), but it shows some drawbacks at smaller scales (galactic, and centre of galaxy clusters scales (Del Popolo and Gambera 2000; Del Popolo 2002; Del Popolo and Cardone 2012; Newman et al. 2013a,b; Del Popolo 2014a)) [1].

Of the main problems of the ΛCDM paradigm the most "stubborn" seems to be the so called Cusp/Core problem (Moore 1994; Flores and Primack 1994)[2] dealing with a discrepancy between the flat density profiles observed in LSBs and dwarf galaxies, and the cuspy density profile obtained in N-body simulations, e.g. the Navarro-Frenk-White (NFW) profile (Navarro et al. 1996b, 1997, 2010). The NFW profile predicts an inner profile going as $\rho \propto r^\alpha$, with $\alpha = -1$. An even steeper profile predicted by Moore et al. (1998) and Fukushige and Makino (2001) gives $\rho \propto r^\alpha$, with $\alpha = -1.5$, while other authors found that the inner slope is dependent on the object considered, and/or its mass (Jing and Suto 2000; Ricotti 2003; Ricotti and Wilkinson 2004; Ricotti et al. 2007; Del Popolo 2010; Cardone et al. 2011b; Del Popolo 2011; Del Popolo et al. 2013d; Di Cintio et al. 2014). More recent N-body dissipationless simulations seem to agree on the fact that a profile flattening towards

[1]For precision sake, the ΛCDM paradigm suffers of other problems even at cosmological scales (e.g., the cosmological constant problem (Weinberg 1989; Astashenok and del Popolo 2012), and the "cosmic coincidence problem").

[2]The other most often mentioned problems of the ΛCDM paradigm, are a) the discrepancy between the number of subhaloes that N-body simulations predict (e.g. Moore et al. 1999) and observations; b) the Too-Big-To-Fail (TBTF) problem. In this last problem simulated haloes have too many, too dense and massive subhalos in comparison to observations (Boylan-Kolchin et al. 2011, 2012). Unified solutions have been proposed to the quoted problems, based on the action of baryons located in the inner parts of the haloes (Zolotov et al. 2012; Del Popolo et al. 2014).

the centre, to a minimum value of $\simeq -0.8$ (Stadel et al. 2009), namely the Einasto profile, seems to be a better fit to simulations (Gao et al. 2008).

The problem is that the smallest value predicted by dissipationless N-body simulations is larger than the values obtained by observations (Burkert 1995; de Blok et al. 2003; Swaters et al. 2003; Kuzio de Naray and Kaufmann 2011; Oh et al. 2011a,b), in SPH simulations (Governato et al. 2010, 2012), or in semi-analytical models (Del Popolo 2009; Cardone and Del Popolo 2012; Del Popolo 2012a,b; Del Popolo and Hiotelis 2014). Recently, Polisensky and Ricotti (2015) found that haloes do not show universal density profiles, rather their shape is determined by the initial linear power spectrum of density perturbations. In addition, the authors found that profiles depend on the halo mass, in agreement with previous works on the subject and that warm dark matter (WDM) halos develop a core, but this is not significant enough to explain observations.

The cusp/core problem has been also noticed at galaxy clusters scales. Kinematics and lensing constraints in cD galaxies (BCG) located in the centre of relaxed clusters, showed that the clusters DM profiles is flatter than a NFW profile, but the total mass profile is in agreement with the NFW predictions (Sand et al. 2002, 2004; Newman et al. 2013a,b).

Dwarf galaxies are dark matter (DM) dominated, and have a low baryon fraction (de Blok and McGaugh 1997). They have been widely used because of their simple dynamical structure, at least disk galaxies without bulges. In the case of high-surface brightness objects (larger objects), it is more complicated to determine the inner density structure. So, the previous statement on the cored nature of the inner density profile of all galaxies, is not at all obvious. While according to Spano et al. (2008) high-surface brightness galaxies are cored, other authors (e.g., Simon et al. 2005; de Blok et al. 2008; Del Popolo and Cardone 2012; Del Popolo et al. 2013d; Martinsson et al. 2013) conclude differently. The THINGS sample shows a tendency to have profiles better described by isothermal (ISO) profiles for low luminosity galaxies, $M_B > -19$ and the profiles are equally well described by cuspy or cored profiles for $M_B < -19$. However, even dwarfs do not always have flat slopes, as shown by Simon et al. (2005). In the case of NGC 2976, 4605, 5949, 5693, 6689, the authors showed that the profiles range from 0 (NGC2976) to -1.28 (NGC5963). Different results have been obtained even using similar techniques for the same object. For example, in the case of NGC2976 the dark matter profile slope is bracketed by $-0.17 < \alpha < -0.01$, according to Simon et al. (2003), while $\alpha = -0.90 \pm 0.15$ for Adams et al. (2012), $\alpha = -0.53 \pm 0.14$ according to Adams et al. (2014), considering stars as tracers, or $\alpha = -0.30 \pm 0.18$ (Adams et al. 2014), considering gas as tracer.

The previous discussion highlights the fact that the determination of the inner slope of galaxies, even dwarves, is not at all an easy task. The result from the previous studies and several others is that exists a range of profiles, and even with the improvements of nowadays kinematic maps there is no agreement on the exact dark matter slopes distribution (Simon et al. 2005; Oh et al. 2011b; Adams et al. 2014).

The situation is even more clear going to larger masses (e.g., spiral galaxies) dominated by stars[3], and especially to smaller masses (e.g. dwarf spheroidals (dSphs)) where biases that enter in the system modelling (Battaglia et al. 2013) lead to opposite results.

Several techniques have been used. The spherical Jeans equation gives results highly dependent on the assumptions, since mass and anisotropy of the stellar orbits are degenerate in the quoted model (Evans et al. 2009). Maximum likelihood in parameter space in Jeans modelling (Wolf and Bullock 2012; Hayashi and Chiba 2012; Richardson and Fairbairn 2013) has similar problems. Schwarzschild modelling has been used for (e.g.) Sculptor and Fornax finding cored profiles (Jardel and Gebhardt 2012; Breddels et al. 2013; Jardel and Gebhardt 2013; Jardel et al. 2013). Methods based on multiple stellar populations concluded that Fornax (slope measured at $\simeq$ 1 kpc) and Sculptor (slope measured at $\simeq$ 500 pc) have a cored profile (Battaglia et al. 2008; Walker and Peñarrubia 2011; Agnello and Evans 2012; Amorisco and Evans 2012). However, a cusp is found in Draco using a Schwarzschild model (Jardel et al. 2013). The previous results show that in reality there is no accepted conclusion on the inner structures of dSphs.

On the other side, a clear determination of the cored or cuspy structure of dSphs is very important because the smaller is the mass of an object the more probable is that its inner profile is similar to that of dissipationless N-body simulations predictions, namely cuspy.

Concerning how the Cusp/Core problem could be solved, there are at least two different approaches:
a) cosmological solutions, based on a different spectrum at small scales (e.g. Zentner and Bullock 2003), different nature of the dark matter particles (Colín et al. 2000; Goodman 2000; Hu et al. 2000; Kaplinghat et al. 2000; Peebles 2000; Sommer-Larsen and Dolgov 2001), or modified gravity theories, e.g., $f(R)$ (Buchdahl 1970; Starobinsky 1980), $f(T)$ (see Bengochea and Ferraro 2009; Linder 2010; Dent et al. 2011; Zheng and Huang 2011) and MOND (Milgrom 1983a,b).
b) Astrophysical solutions. These are based on the idea that the dark matter component of a galaxy expands due to a "heating" mechanism with the result that the inner density is reduced.

The two most known astrophysical solutions are a) "supernovae feedback flattening" (SNFF) of the cusp (Navarro et al.

[3] See Section 3 for a wider discussion.

1996a; Gelato and Sommer-Larsen 1999; Read and Gilmore 2005; Mashchenko et al. 2006, 2008; Governato et al. 2010, 2012),
and
b) "dynamical friction from baryonic clumps" (DFBC) (El-Zant et al. 2001, 2004; Ma and Boylan-Kolchin 2004; Nipoti et al. 2004; Romano-Díaz et al. 2008, 2009; Del Popolo 2009; Cole et al. 2011; Inoue and Saitoh 2011; Nipoti and Binney 2015).

A wider discussion of the two models is given in Sections 2.2.1 and 2.2.2. Here, we may recall that the SNFF model in the Governato et al. (2010) results has been found in agreement with the THINGS galaxies (de Blok et al. 2008; Walter et al. 2008) density profiles (Oh et al. 2008, 2011a,b). Results somehow contradicting the previous ones are those of (e.g.) Trujillo-Gomez et al. (2015) who simulated feedback from supernovae (SN) and radiation pressure from massive stars, both in disk galaxies and dwarfs. They found that the second effect is more important than supernovae feedback. The ability of the model to solve the small scale problems of the ΛCDM model has also been questioned by several authors (Ferrero et al. 2012; Peñarrubia et al. 2012; Garrison-Kimmel et al. 2013, 2014; Papastergis et al. 2015) (see Section 2.2.1).

The DFBC predicted the correct shape of galaxy density profiles (Del Popolo 2009; Del Popolo and Kroupa 2009) in agreement with the SPH simulations performed by Governato et al. (2010, 2012) and of clusters (Del Popolo 2012a) by Martizzi et al. (2012) and as well predicted correlations among several quantities observed in clusters of galaxies (Del Popolo 2012a), later observed in Newman et al. (2013a,b).

Recently, Di Cintio et al. (2014) showed that the inner slope depends on the ratio $M_*/M_{\rm halo}$ in the SNFF scheme. A more detailed discussion of the model is performed in Section 2.2.1. It predicts a dependence of the inner slope from the ratio $M_*/M_{\rm halo}$. The profile goes from a cuspy one for low values of the quoted ratio to cored ones and again to a cuspy one for large spiral galaxies. We want to recall that in the DFBC scheme it was found a correlation among the inner slope, the halo mass and the angular momentum of the structure (Del Popolo 2009, 2010, 2012a,b), in the case of dwarf galaxies, normal spirals, and clusters. In clusters, a series of other correlation were found (Del Popolo 2012b), namely a) a correlation among the inner slope and baryonic content to halo mass ratio at $z=0$, $M_{\rm b}/M_{500}$, and at $z_{\rm initial}$, $M_{\rm b,in}/M_{500}$ (see Del Popolo 2012b, their figures 2, 4)[4], and angular momentum[5]. We recall that the baryonic mass $M_{\rm b,in}$ is the initial gas content of the protostructure, while $M_{\rm b}$ is the final baryonic content, namely $M_{\rm b}=M_{\rm gas+stars}$. Another confirmation of the goodness of the DFBC is that the inner slope dependence on the ratio $M_*/M_{\rm halo}$ is similar to SPH simulations results, although in the case of clusters and for a different mechanism than that of SPH simulations. b) In the cluster case, a further correlation between the inner slope and the Brightest Cluster Galaxy (BCG) mass, the core radius $r_{\rm core}$ and the effective radius $R_{\rm e}$, and another correlation between the mass inside 100 kpc, which is mainly dark matter, and that inside 5 kpc, mainly constituted by baryons (Del Popolo 2014b) was found (see also Del Popolo 2012b).

Moreover, it was shown that the DFBC mechanism is able to explain the flattening in dwarves as well in clusters (Del Popolo 2009, 2012a, 2014a).

In the following, we want to compare the predictions of the SNFF mechanism with the DFBC. To this aim, we will use the results of Di Cintio et al. (2014), and compare those results with the observations of Adams et al. (2014), THINGS galaxies, and dwarves, LITTLE THINGS, Sculptor, Fornax, and the Milky Way (MW).

The paper is organized as follows. In Section 2 we describe the data used and the models that we compare to the data. Sections 3 and 4 are devoted to results and conclusions, respectively. Finally in the appendix A we discuss in detail the DFBC mechanism.

2 Models and data

In the present paper, we will try to discern among the two previously quoted astrophysical mechanisms that are able to give rise to cored galaxies. Conscious of the limitations in the determination of the inner slope of the density profile α, we will use the best data nowadays available.

2.1 Data

The data that we will use are those based on "high resolution integral field spectroscopy" of seven nearby galaxies, namely NGC0959, UGC02259, NGC2552, NGC2976, NGC5204, NGC5949, UGC11707, obtained by Adams et al. (2014) through measurements of their gas kinematics and integrated stellar light. The complete description of the sample selection, photometry, integral field spectroscopy, kinematic extraction of gas and stars are discussed in detail in Adams et al. (2014). The dynamical parameters of the galaxies were obtained using Bayesian statistics, and differently from other studies (e.g., dwarf galaxies in Oh et al. 2011a,b) the entire dark matter density profiles were fitted with a Burkert profile (Burkert 1995)

$$\rho(r)=\frac{\rho_{\rm b}}{(1+r/r_{\rm b})(1+(r/r_{\rm b})^2)}\ , \qquad (1)$$

[4] M_{500} is the mass in R_{500}, the radius enclosing a density 500 times larger than the critical one

[5] Since the angular momentum acquired is inversely proportional to the peak height (Del Popolo and Gambera 1996; Del Popolo 2009), the collapse of larger mass structures is slowed down

Table 1 Galaxy sample properties from Adams et al. (2014). The upper (lower) part refers to the gas (star)-tracer data.

Galaxy	α	$\log_{10} M_*$ $/M_\odot$	$V_{\rm rot}$ km/s	Υ_*	$\log_{10} M_{200}$ $/M_\odot$	$\log_{10} L$ $/L_\odot$
NGC 959	-0.88 ± 0.15	$(0.94^{+0.12}_{-0.13}) \times 10^9$	$59.86^{+2.19}_{-2.42}$	1.10 ± 0.15	11.06 ± 0.23	8.93
UGC 2259	-0.72 ± 0.09	$(0.25^{+0.06}_{-0.07}) \times 10^9$	$41.077^{+2.683}_{-3.227}$	1.07 ± 0.27	11.42 ± 0.14	8.36
NGC 2552	-0.38 ± 0.11	$(1.3^{+0.2}_{-0.27}) \times 10^9$	$65.23^{+3.25}_{-3.7}$	1.01 ± 0.19	11.33 ± 0.11	9.10
NGC 2976	-0.30 ± 0.18	$(0.79 \pm 0.21) \times 10^9$	$57.13^{+3.87}_{-4.74}$	0.83 ± 0.22	11.94 ± 0.51	8.98
NGC 5204	-0.85 ± 0.06	$(0.25 \pm 0.03) \times 10^9$	$41.45^{+1.35}_{-1.46}$	1.08 ± 0.13	11.36 ± 0.16	8.37
NGC 5949	-0.53 ± 0.14	$(2.98^{+0.92}_{-0.88}) \times 10^9$	$82.89^{+6.31}_{-7.7}$	1.16 ± 0.34	11.82 ± 0.42	9.41
UGC 11707	-0.41 ± 0.11	$(1.2^{+0.3}_{-0.24}) \times 10^9$	$64.4^{+3.5}_{-4.02}$	1.11 ± 0.23	11.49 ± 0.18	9.04
NGC 959	-0.73 ± 0.10	$(0.92 \pm 0.23) \times 10^9$	$59.55^{+3.86}_{-4.62}$	1.08 ± 0.27	11.64 ± 0.32	8.93
UGC 2259	-0.77 ± 0.21	$(0.25 \pm 0.1) \times 10^9$	$41.4^{+4.1}_{-5.54}$	1.10 ± 0.44	11.62 ± 0.61	8.36
NGC 2552	-0.53 ± 0.21	$(1.6^{+0.7}_{-0.73}) \times 10^9$	$69.11^{+7.51}_{-10.5}$	1.24 ± 0.55	11.23 ± 0.38	9.10
NGC 2976	-0.53 ± 0.14	$(0.89^{+0.21}_{-0.20}) \times 10^9$	$58.98^{+3.47}_{-4.09}$	0.93 ± 0.21	11.56 ± 0.46	8.98
NGC 5204	-0.77 ± 0.19	$(0.30 \pm 0.1) \times 10^9$	$43.67^{+3.57}_{-4.54}$	1.30 ± 0.42	11.76 ± 0.51	9.37
NGC 5949	-0.72 ± 0.11	$(3.1 \pm 0.7) \times 10^9$	$83.68^{+5.08}_{-6.02}$	1.20 ± 0.28	11.46 ± 0.22	9.41
UGC 11707	-0.65 ± 0.26	$(1.2^{+0.5}_{-0.51}) \times 10^9$	$63.78^{+6.48}_{-8.82}$	1.07 ± 0.44	11.13 ± 0.37	9.04

and a generalized NFW (gNFW) profile (Zhao 1996):

$$\rho(r) = \frac{\delta_{\rm c}\rho_{\rm c}}{(r/r_{\rm s})^{\alpha}[1+(r/r_{\rm s})]^{3-\alpha}} \ , \qquad (2)$$

where

$$\delta_{\rm c} = \frac{200}{3}\frac{c^3}{\zeta(c,\alpha,1)} \ , \qquad (3)$$

$\rho_{\rm c}$ is the critical density and c the concentration parameter. The function $\zeta(c,\alpha,q_{\rm h})$ is defined as (Barnabè et al. 2012):

$$\zeta(c,\alpha,q_{\rm h}) = \int_0^c \frac{\tau^{2-\alpha}(1+\tau)^{\alpha-3}}{\sqrt{1-(1-q_{\rm h}^2)\tau^2/c^2}}\,{\rm d}\tau \ , \qquad (4)$$

where $q_{\rm h}$ indicates the 3D axial ratio of the profile. For spherical symmetry, $q_{\rm h} = 1$ as in Eq. 3.

The complete list of parameters in the study is listed in table 4 of Adams et al. (2014), and apart the DM parameters, the gas-based parameters contain a stellar anisotropy term β_z that is used as a free parameter in the "Jeans Anisotropic Multi-Gaussian-Expansion" models (Cappellari 2008). The parameters were constrained by using gas and stars as tracers.

In table 1, we report the galaxy name, the slope α, M_*, $V_{\rm rot}$, the mass-to-light ratio Υ_*, M_{200} and the luminosity L. The stellar mass M_* is calculated from the luminosity and Υ_*, while the circular velocity at 2.2 disc scale-lengths $V_{\rm rot}$ is calculated by means of the stellar mass Tully-Fisher (TF) relation (Eq. 4 of Dutton et al. (2010)):

$$\log\frac{V_{2.2}}{\rm km/s} = 2.143 + 0.281\left(\log\frac{M_*}{10^{10}h^{-2}M_\odot}\right) \ , \qquad (5)$$

where $V_{2.2} = V_{\rm opt}$. We chose this equation because, as we will see later, it was used by Di Cintio et al. (2014) in converting M_* to $V_{\rm rot}$ (the rotational velocity) in their figure 6.

Another data set comes from the THINGS dwarfs studied by Oh et al. (2011a,b). The detailed description of the parameters of interest to our work and the slope α can be found in Oh et al. (2008, 2011a,b). Summarizing, they used high-resolution HI data from the THINGS survey [6]. They selected 7 dwarf galaxies with clear rotation pattern from THINGS in order to obtain the rotation curves. In order to extract the velocity field from the data cube, different techniques can be used (Intensity-Weighted Mean (IWM) velocity field; peak velocity fields; single, multiple Gaussian or Hermite polynomial fits). In order to take appropriately into account multiple velocity components, non-circular motions, and so on, Oh et al. (2008) introduced a new method to extract from the HI data cube the circularly rotating components, the so called "bulk-motion extraction method". Since a rotation curve incorporates the dynamics of gas, stars and dark matter, in order to obtain the dynamics of the dark matter, it is necessary to extract the baryons contribution from the total dynamics. The stellar component mass models are obtained deriving the galaxies luminosity profiles through a tilted ring modelling applied to the SINGS 3.6 μm images to obtain the surface brightness profiles. The luminosity profiles are then converted into mass density profiles using a Υ_* empirical relation, obtained from population synthesis models. The HI surface density profile is obtained from the column density of HI, and the tilted-ring model applied to the HI maps gives the radial HI distribution. By subtracting the baryons dynamics to the total one, it is possible to obtain the dark matter mass model of the galaxies. The halo models used are the NFW and the ISO profiles.

[6] THINGS was a HI survey program undertaken with VLA comprising 34 nearby galaxies with high spectral ($\leq$ 5.2 km/s), and spatial ($6''$) resolution. 3.6 μm data, with $4''$ resolution, from SINGS (Spitzer Infrared Nearby Galaxies Survey) (Kennicutt et al. 2003), were used to constrain the stellar component contribution to the total kinematics.

The last profile is given by

$$\rho(r) = \frac{\rho_0}{1 + (r/r_c)^2} \quad (6)$$

where r_c is the core radius, and ρ_0 the halo central density.

Using different prescriptions for Υ_*, one can obtain a "maximum disk", a "minimum disk", etc., fit to the rotation curve. The density profile can be obtained from the Poisson equation (de Blok et al. 2001):

$$\rho(R) = \frac{1}{4\pi G}\left[2\frac{V}{R}\frac{dV}{dR} + \left(\frac{V}{R}\right)^2\right] , \quad (7)$$

Finally, the inner slope is obtained determining the position where the slope changes most rapidly (break radius). A least-squares fit to the inner points to the break radius (usually 5 points) gives α. The uncertainty is calculated recalculating the slope excluding the data point at the break radius, and including the first point outside the break radius. The error $\Delta\alpha$ is defined as the difference among these slopes. Note again that the value of α, in this case, was obtained only using the inner points and not the entire density profile as in Adams et al. (2014).

In table 2, we show the values of α, M_*, and $V_{\rm rot}$ for ICG2574, NGC2366, Ho I, Ho II, M81 dwB, DD0153, DD0 154 (see table 1 of Oh et al. 2011a).

The same technique previously described can be applied to dwarf galaxies from "Local Irregulars Trace Luminosity Extremes, The HI Nearby Galaxy Survey" (LITTLE THINGS). In table 3, we reproduce α, M_*, and $V_{\rm rot}$ for a smaller sample of the quoted dwarfs, kindly provided by Se-Heon Oh (Oh et al. 2015).

Finally, in table 4, we present M_* from the THINGS spirals, their $V_{\rm rot}$ obtained with the Dutton et al. (2010) formula, and the α values obtained from the rotation curve of the quoted galaxies. These data were kindly provided by Se-Heon Oh. Another determination of the slopes of the THINGS galaxies was performed by Chemin et al. (2011) (see Section 3 for a wider discussion).

In our analysis we also used the Simon et al. (2005) galaxies not re-studied in Adams et al. (2014) (see table 5).

Table 2 Galaxy sample properties for THINGS dwarfs from Oh et al. (2011a).

Galaxy	α	M_* ($M_\odot$)	$V_{\rm rot}$ (km/s)
IC 2574	$+0.13 \pm 0.07$	10.38×10^8	77.6
NGC 2366	-0.32 ± 0.10	2.58×10^8	57.5
Holmberg I	-0.39 ± 0.06	1.25×10^8	38.0
Holmberg II	-0.43 ± 0.06	2.00×10^8	35.5
M81 dwB	-0.39 ± 0.09	0.30×10^8	39.8
DDO 53	-0.38 ± 0.06	0.18×10^8	32.4
DDO 154	-0.29 ± 0.15	0.26×10^8	53.2

Table 3 Galaxy sample properties for LITTLE THINGS (Oh et al. 2015).

Galaxy	α	$\log_{10} M_*/M_\odot$	$V_{\rm rot}$ (km/s)
DDO 210	-0.70 ± 0.04	5.602	6.75
UGC 8508	-0.38 ± 0.16	6.477	11.9
CVnIdwA	0.03 ± 0.27	6.612	12.98
DDO 216	-0.03 ± 1.30	6.934	15.98
WLM	0.02 ± 0.02	7.090	17.71
DDO 70	-0.48 ± 0.02	7.093	17.72
IC 1613	-0.10 ± 0.92	7.288	20.14
DDO 126	-0.39 ± 0.05	7.356	21.05
DDO 133	-0.11 ± 0.16	7.418	21.9
DDO 168	0.62 ± 0.36	7.710	26.47
DDO 101	-1.02 ± 0.12	7.730	26.81
HARO36	-0.50 ± 0.02	7.764	27.33
DDO 87	-0.01 ± 0.48	7.791	27.87
DDO 52	-0.49 ± 0.02	7.857	29.16
DDO 50	0.10 ± 0.41	7.991	31.7
NGC 2366	-0.34 ± 0.10	8.034	32.64
IC 10	-0.25 ± 0.32	8.072	33.46
NGC 3738	-0.44 ± 0.03	8.096	34.89
NGC 1569	-0.23 ± 0.67	8.316	39.14

Table 4 Galaxy sample properties for spiral THINGS (disks) (Oh et al. 2015).

Galaxy	α	$\log_{10} M_*/M_\odot$	$V_{\rm rot}$ (km/s)
NGC7331	-1.19	11.26	263.2
NGC3031	-0.80	10.91	209.8
NGC6946	-0.70	10.79	195.4
NGC3198	-0.40	10.49	159.9
NGC3521	-0.10	11.09	235.8
NGC2403	-0.70	9.71	96.5
NGC7793	-0.70	9.44	81.1
NGC4736	-1.0	10.35	146.1
NGC3621	-0.9	10.29	140.5
NGC2841	-1.8	11.13	241.95
NGC2903	-2.0	10.21	133.4

Simon et al. (2005) performed an analysis of dwarf and LSB galaxies based on Hα high-resolution velocity fields for the galaxies NGC 5963, NGC 6689, NGC 4605, and NGC 5949. In the case of NGC 5963 and NGC 4605, CO velocity fields were studied. In order to avoid the usual problems connected to the long-slit spectroscopy (Simon et al. 2003; Swaters et al. 2003) in the RCs determination, they used two-dimensional velocity fields. Multiple wavelengths velocity fields (e.g., CO, and Hα) were obtained in order to further reduce systematic errors. Multi-color imaging was also used to improve stellar mass-to-light ratio determination. This improves the step of modelling and removing the stellar disk. By means of the photometry they measured geometric parameters, and used the routine RINGFIT (i.e., tilted-ring modelling) to obtain the radial velocity of the system and RCs starting from the velocity fields (see Simon et al. 2003, 2005, for a detailed analysis).

Finally, we show the density slope α, the mass of the stellar component M_* and the maximum velocity $V_{\rm rot}$ for the Milky Way, Fornax and Sculptor in table 6.

A further comment regarding the data used is at this point necessary. When we only know the stellar mass M_* of the object considered and we need to infer the rotation velocity $V_{\rm rot}$, we used the relation given by Dutton et al. (2010). We therefore checked the reliability of this relation with objects where both the stellar mass and the rotational velocity is known. We noticed though that for some points the velocities inferred differ from the true one and therefore few points in the $\alpha - M_*$ plot are in a different position with respect to the same points in the $\alpha - V_{\rm rot}$ plot. Since this is not a systematic effect, we assume nevertheless the validity of the Dutton et al. (2010) relation acknowledging the fact that some uncertainties still hold.

2.2 Models

2.2.1 Supernovae feedback flattening

The models we want to compare data with are the two already discussed mechanisms of cusp flattening, namely the "supernovae feedback flattening" (SNFF) model (Navarro et al. 1996a; Gelato and Sommer-Larsen 1999; Read and Gilmore 2005; Mashchenko et al. 2006, 2008; Governato et al. 2010, 2012; Teyssier et al. 2013), and the "dynamical friction from baryonic clumps" model (DFBC) (El-Zant et al. 2001, 2004; Ma and Boylan-Kolchin 2004; Nipoti et al. 2004; Romano-Díaz et al. 2008; Del Popolo 2009; Romano-Díaz et al. 2009; Cole et al. 2011; Inoue and Saitoh 2011; Nipoti and Binney 2015).

The importance of baryons in solving the Cusp/Core problem was suggested starting from Flores and Primack (1994) and stressed in many following works. The first mechanism envisaged was connected to supernovae feedback.

Navarro et al. (1996a) showed that the sudden expulsion of baryons into the halo in a single event could flatten the profile. However, Gnedin and Zhao (2002) showed that a single explosive event has not sufficient energy to form a core, while repeated moderate violent explosions could reach the goal (however see Garrison-Kimmel et al. (2013) for a different point of view). Mashchenko et al. (2006, 2008) showed that in primordial galaxies, random bulk motions of gas driven by SN explosions could form a core, and a similar model by Governato et al. (2010) found the same result. Oh et al. (2011a,b) compared the average slope of THINGS dwarves with the simulations by Governato et al. (2010), and Governato et al. (2012) made a similar comparison for larger objects, and found a correlation among M_* and the inner slope for galaxies having $M_* > 10^6 M_\odot$ [7]. The Governato's papers used the code GASOLINE (Wadsley et al. 2004), a N-Body+SPH code to simulate galaxies. By means of the "zoom" technique (Katz and White 1993), the resolution for gas particles was $M_{\rm p,gas} = 3 \times 10^3 M_\odot$, and $M_{\rm p,DM} = 1.6 \times 10^4 M_\odot$ for DM particles, and the softening 86 kpc. The authors performed a run in which stars formed if the hydrogen density was $> 100/{\rm cm}^3$ (High Threshold (HT) run), and another in which stars formed if the hydrogen density was $> 0.1/{\rm cm}^3$ (Low Threshold (LT) run).
These simulations, similarly to Di Cintio et al. (2014), implement SN feedback through the blast wave SN feedback (Stinson et al. 2006), and/or early stellar feedback (Stinson et al. 2013). Stars with masses larger than $8\ M_\odot$ deposit an energy of 10^{51} erg in the interstellar medium (ISM). Even metals are allowed to diffuse between the particles of gas (Shen et al. 2010). The coupling of energy eject from SN to the ISM is obtained using a coupling coefficient $\epsilon_{\rm esf}$. In the MaGICC simulations (Stinson et al. 2013)

[7] In Galaxies with $M_* < 10^6 M_\odot$ the supernovae feedback mechanism was not able to transform cusps into cores.

Table 5 Galaxy properties from the Simon et al. (2005) sample.

Galaxy	α	M_* ($M_\odot$)	$V_{\rm rot}$ (km/s)
NGC4605	-0.78 ± 0.04	2×10^9	74
NGC5963	-1.20 ± 0.13	9.3×10^9	114
NGC6689	-0.79 ± 0.12	4.5×10^9	94

Table 6 Galaxy sample properties for Milky Way (Ascasibar et al. 2006), Fornax and Sculptor (Walker and Peñarrubia 2011).

Galaxy	α	M_* ($M_\odot$)	$V_{\rm rot}$ (km/s)
Milky Way	-1.03 ± 0.04	$(6.43 \pm 0.63) \times 10^{10}$	$196.5^{+3.6}_{-3.8}$
Fornax	$-0.39^{+0.43}_{-0.37}$	$(3.12 \pm 0.35) \times 10^7$	17.8 ± 0.7
Sculptor	$-0.05^{+0.51}_{-0.39}$	$(8 \pm 0.7) \times 10^6$	$17.3^{+2.2}_{-2.0}$

the fiducial $\epsilon_{\rm esf} = 0.1$. In the following (Sect. 2.2.3), we will discuss more in detail the coupling parameters (e.g., Peñarrubia et al. 2012).

Di Cintio et al. (2014), using the same code (GASOLINE), and similar parameters showed that if $M_*/M_{\rm halo} \leq 0.01\%$ the stellar feedback energy is not enough to turn cusps into cores, and one expects cuspy profiles similar to the NFW or more cuspy. Going up with stellar mass (better $M_*/M_{\rm halo}$) the profiles become less steep, and when the ratio $M_*/M_{\rm halo} \simeq 0.5\%$ one gets the flattest profiles. For a larger $M_*/M_{\rm halo}$ ratio the deepening of the potential well of the galaxies, produced by a larger number of stars, opposes the SNFF mechanism and galaxies have more cuspy profiles. Di Cintio et al. (2014) used the stellar mass Tully-Fisher (TF) relation (Eq. 4 of Dutton et al. 2010) to have predictions on the DM inner slope on the galaxies observed rotation velocity. The model predicts that the galaxies in which the cored profiles should be more evident are LSB galaxies (in agreement with observations, de Blok et al. 2008; Oh et al. 2011a), while in small velocity (mass) dSphs the profiles tend to be cuspy. The situation is more complicated for disk galaxies of larger mass (e.g., Milky Way) which are baryon dominated and the uncertainties in the disc-halo decomposition are larger. For those galaxies it is difficult to have a clear cut on the cuspy or cored nature of the density profile. As already discussed, for larger mass galaxies ($V_{\rm rot} > 150$ km/s), de Blok et al. (2008) and Martinsson et al. (2013) showed that ISO or NFW fit equally well the density profiles. Other studies (e.g., Donato et al. 2004; McGaugh et al. 2007) reached the conclusion that cored profiles describe well the density profile.

2.2.2 *Gas clumps merging*

As already reported, the other mechanism able to transform cusps into cores is that proposed by El-Zant et al. (2001, 2004)[8], based on merging gas clumps of $10^5 M_\odot$ in the case of dwarves, and $10^8 M_\odot$ in the case of spirals[9]. Energy and angular momentum transfer from clumps to DM can flatten the profile, and the process is the more efficient, the earlier it happened, when halos were smaller. The effectiveness of the process has been confirmed by several authors (Ma and Boylan-Kolchin 2004; Nipoti et al. 2004; Romano-Díaz et al. 2008; Del Popolo 2009; Romano-Díaz et al. 2009; Cole et al. 2011; Inoue and Saitoh 2011; Del Popolo et al. 2014; Nipoti and Binney 2015).

More in detail, as shown in Del Popolo (2009); Del Popolo et al. (2014), initially the proto-structure is in the linear phase, containing DM and diffuse gas. The proto-structure expands to a maximum radius and then re-collapses, first in the DM component that forms the potential well in which baryons will fall. Baryons subject to radiative processes form clumps, which collapse to the centre of the halo while forming stars (De Lucia and Helmi 2008; Li et al. 2010, (see Sect. 2.2.2, 2.2.3)). In the collapse phase baryons are compressed (adiabatic contraction (Blumenthal et al. 1986; Gnedin et al. 2004)), so making more cuspy the DM profile. The clumps collapse to the galactic centre, because of dynamical friction (DF) between baryons and DM, transferring energy and angular momentum to the DM component. The cusp is heated, and a core forms, before stars form and stellar feedback starts to act expelling a large part of the gas, leaving a lower stellar density with respect to the beginning. Feedback destroys clumps[10] soon after a small part of their mass is transformed into stars. The mass distribution is then dominated by DM.

The model described is in agreement with El-Zant et al. (2001, 2004); Ma and Boylan-Kolchin (2004); Nipoti et al. (2004); Romano-Díaz et al. (2008, 2009); Cole et al. (2011); Inoue and Saitoh (2011); Nipoti and Binney (2015).
It is the only model able to explain the correct dependence of the inner slope of the DM profile over 6 order of magnitudes in the halo mass, namely from dwarves to clusters (Del Popolo 2009, 2010, 2012a,b, 2014a). Here we want to stress another interesting point. As previously reported the model showed that the inner slope is mass dependent (Del Popolo 2009, 2010, 2012a,b). Moreover in Del Popolo (2012b) and Del Popolo (2014b) were found correlations among the inner slope and other quantities with the BCG mass and radius, in agreement with results by Newman et al. (2013a,b).

2.2.3 *Drawbacks and differences between the models*

As already described, the SNFF model is based on the expulsion of gas due to SN explosions, while the DFBC model is based on dynamical friction between baryons and DM. The two models work in a different way. In the case of the SNFF model we start from gas which forms stars which can then explode into SN if they posses the correct mass. So, in this model in order to produce the density profile flattening, we need a longer and more complex series of events to reach the goal (cusps transformed into cores). In the case of the DFBC, it is enough that big gas clumps are present to flatten the density profile. In a few words, the DFBC model is more ergonomic than the SNFF model.

In the last years, it has been shown that the SNFF model has some drawbacks. Peñarrubia et al. (2012) calculated the

[8] For precision's sake, the concept that large clouds could heat stellar systems was proposed by Spitzer and Schwarzschild (1951).

[9] In the Nipoti and Binney (2015) simulations, the clump mass was $10^5 - 10^6 M_\odot$, and the total mass $10^9 M_\odot$.

[10] This is allowed since star formation is a not efficient process.

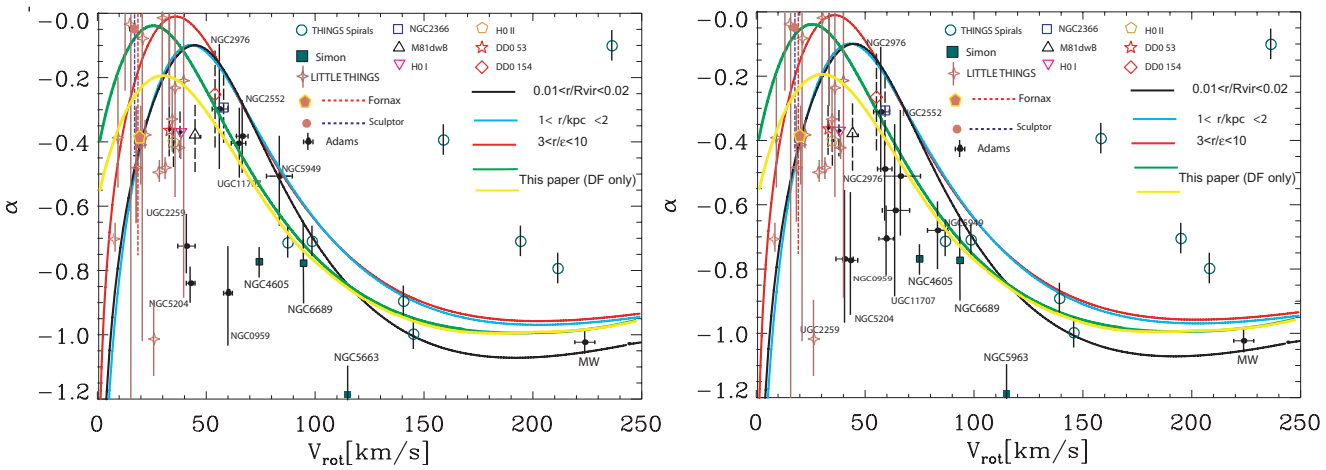


Fig. 2 The α-$V_{\rm rot}$ relation compared to observations. Data come from Adams et al. (2014), Simon et al. (2005) (excluding the galaxies studied by Adams et al. (2014)), the THINGS spirals, the THINGS dwarves, the LITTLE THINGS, Fornax, and Sculptor (Walker and Peñarrubia 2011) and the MW (Ascasibar et al. 2006). The red, black, and blue lines describe the model of Di Cintio et al. (2014), while the green and yellow lines the model of the present paper. The only difference between the left and right panel is due to the galaxy sample in Adams et al. (2014): gas traced, in the left panel; stellar traced, in the right panel. The green (yellow) curves are our equivalent for the red (cyan) curve of Di Cintio et al. (2014).

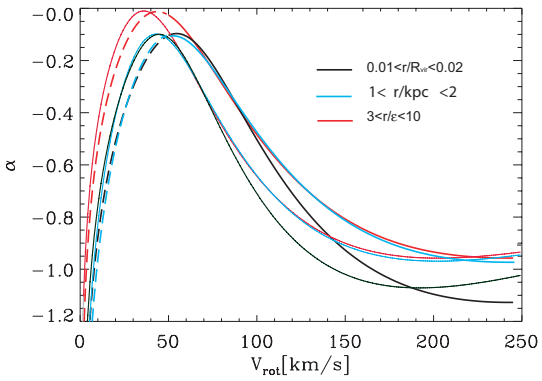


Fig. 1 The α-$V_{\rm rot}$ relation. The dashed lines refer to the calculations of Di Cintio et al. (2014), and the solid lines are those calculated in this paper. The dashed lines and the solid ones are different by a factor h inverse, coming from the Tully-Fisher relation of Dutton et al. (2010), and discarded in Di Cintio et al. (2014). The black lines refer to the slope calculated at $0.01 < r/R_{\rm vir} < 0.02$, the cyan lines that calculated at $1 < r/{\rm kpc} < 2$ and the red lines refer to the slope calculated at $3 < r/\epsilon < 10$.

energy that SN must inject into the haloes in order to remove the cusp. According to Peñarrubia et al. (2012), in order to transform a cuspy profile into a cored one in MW dSphs, an energy in the range $10^{53} - 10^{55}$ erg is required. The average energy released in a SNII explosion is of the order of 10^{51} erg (Utrobin and Chugai 2011). So the explosions of hundreds to several thousands of SNs could in principle produce this huge amount of energy. However, the low star formation efficiency in dSphs, suggested by their luminous satellites abundance, implies that the real contribution to the energy could be lower than that needed to flatten a profile. Moreover, while the solution to the cusp/core problem with the SNFF model needs a large number of SNs, and so a large star formation efficiency (SFE), the solution of another small scale problem of the ΛCDM model, namely the TBTF problem, places an opposite demand on the SFE. In order to eliminate such a tension one or more of the following issues should be true: a) a coupling of energy coming from SN II to DM of the order of 1. Such a value of the "energy coupling" ($\epsilon_{\rm SN}$) contradicts observations. In order to describe the metallicity-luminosity relation in dSphs, Revaz and Jablonka (2012) obtained a value of $\epsilon_{\rm SN} \simeq 0.05$, while the value of $\epsilon_{\rm SN}$ used in Governato et al. (2010) is 0.40. Even this large value is smaller than what needed to eliminate the quoted tension. b) Cusp removal at high redshifts ($z > 6$ from the Sculptor and Fornax cored profiles). Namely, star formation should peak at redshifts unexpectedly high ($z > 6$). This conclusion is at odds with the fact that star formation went on for 12-13 Gyr in Fornax (de Boer et al. 2012a), and for 6-7 Gyr in Sculptor (de Boer et al. 2012b). Even if the star formation peak was at that redshift, the tension moves

to haloes embedding less stars, the formation of cores in dSphs with $M_* < 10^7 M_\odot$ requires $\epsilon_{\rm SN} \simeq 1$. c) A top-heavy stellar initial mass function. d) Considerable satellite disruption (e.g., by tidal torques). This last issue is promising in the solution of the previously discussed problem as shown by Zolotov et al. (2012); Del Popolo et al. (2014); Brook and Di Cintio (2014); Del Popolo and Le Delliou (2014).

However, we should add that Governato et al. (2010) had to use a very high star formation threshold to obtain their results. Sawala et al. (2014) showed that the high threshold assumption is not necessary to obtain the results claimed by Governato et al. (2010).

One additional argument of discussion about simulations and the TBTF problem is given by Polisensky and Ricotti (2014). The authors could largely reconcile the discrepancy between simulations and observations by using the latest cosmological parameters provided by the WMAP and Planck team. They concluded therefore that the strong tension observed in previous works on the subject was mainly due to the incorrect assumption of the cosmological parameters. Another source of tension comes from the assumed mass of the Milky Way: assuming its most recent estimates, the need of baryonic physics necessary to decrease the density of the most massive satellites in the Milky Way becomes much less compelling. Despite this improvement, one more aspect lacks a satisfactory explanation, namely the problem of missing bright satellites just outside the Milky Way virial radius, as discussed in Bovill and Ricotti (2011a), Bovill and Ricotti (2011b) and Garrison-Kimmel et al. (2013).

On a similar line, Garrison-Kimmel et al. (2013) discuss general problems of the SNFF model and in particular problems in solving the TBTF problem. Comparing the effects of blow-outs of different masses ($10^7 M_\odot$, $10^8 M_\odot$ and $10^9 M_\odot$) they found that a single blow-out of a fixed mass has more effect in changing the structure of a dwarf in comparison with several repeated blow-outs whose mass sums to the that of the single blow-out[11], contrarily to the SNFF model which requires repeated blow-outs (see Governato et al. 2010, 2012; Pontzen and Governato 2012). From the point of view of the mass, for the high resolution simulations of Garrison-Kimmel et al. (2013) to have subhaloes density in line with that observed in MW dSphs, a quantity of mass equal to $10^9 M_\odot$ should be ejected, which is marginally exceeding the baryon content of the dSphs. From the energy point of view, since the average energy emitted by SNs explosions is 10^{51} erg, to match the density of a $10^6 M_\odot$ dSph, the energy of 40000 supernovae is needed with an efficiency of 100%. For six of the nine classical dSphs, this quantity exceeded the number of Type II SN explosions expected. Moreover, they find that explosions can flatten the inner slope to $\alpha > -0.5$, never producing a real core with constant density, as predicted by the last versions of the SNFF model (e.g., Pontzen and Governato 2012). Ferrero et al. (2012) and Papastergis et al. (2015) arrived to similar conclusions, namely the high improbability for the SNFF to solve the TBTF problem. Finally, as several authors noticed (Choi et al. 2014; Laporte and Peñarrubia 2015; Laporte and White 2015; Marinacci et al. 2014), nowadays hydrodynamical simulations have not the required resolution to follow the feedback processes which should transform the cusp into a core.

Finally Oman et al. (2015) and Oman et al. (2016) with the use of hydrodynamical simulations investigate the 'cusp versus core' problem and conclude that this is better characterized as an 'inner mass deficit' problem rather than as a density slope mismatch. Investigating simulated dwarf galaxies and comparing their properties with a selected catalogue of observed galaxies, they find several discrepancies. The authors conclude that to solve these discrepancies, it is necessary either to change the dark matter physics, that the mass profiles of the galaxies giving rise to the 'cusp versus core' problem are incorrect when inferred from kinematic data or that simulations fail to reproduce correctly observations, as pointed by other authors before.

Concerning the DFBC model, to our knowledge there are not studies on its limits. However, since the effectiveness of this process depends on the clumps properties and that of the halo, one could speculate about the a) the origin of the clumps, and b) the time-scales for the density flattening in comparison with the life of the clumps.

Concerning the first issue, some galaxies ("clump clusters" and "chain galaxies") at high redshift show clumpy structures (e.g. van den Bergh et al. 1996; Elmegreen et al. 2004, 2009; Genzel et al. 2011). At $t < 2$ Gyr, when the gas is infalling towards the disc, radiative cooling induces a self-gravity instability which leads to clumps formation (e.g. Noguchi 1998, 1999; Agertz et al. 2009; Bournaud et al. 2009; Ceverino et al. 2010), and finally to the formation of disc galaxies.

Concerning the second issue, as shown by Nipoti and Binney (2015), the flattening process, $t_{\rm flat}$, happens on the dynamical friction scale $t_{\rm fric} \simeq 1.4 t_{\rm cross}/\ln\Lambda$, with $t_{\rm cross} \simeq 21$ Myr, namely the time-scale is very short.

At the same time, in order for the mechanism to work, the gas clumps should live for a time longer than that needed to redistribute DM in the halo centre. The evaluation of this life-time is not easy, since it is connected to a poorly known subject, namely the process of star formation and feedback (e.g. Murray et al. 2010; Genel et al. 2012; Hopkins et al. 2012; Bournaud et al. 2014). The star formation time must be larger than $max[t_{\rm dyn}, t_{\rm cool}]$, where $t_{\rm dyn} = 1/\sqrt{G\rho_{\rm gas}}$

[11] However, repeated blow-outs remove mass preferentially from the centre.

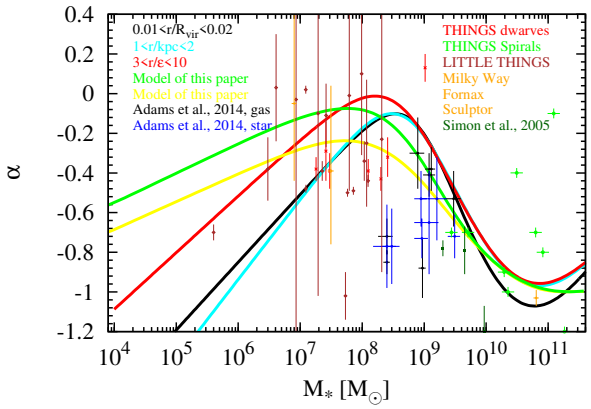


Fig. 3 The α vs. M_* relation. Symbols are like in figure 2, except for the points representing the two samples from Adams et al. (2014): in black we show the gas-traced sample while in blue the stellar-traced sample.

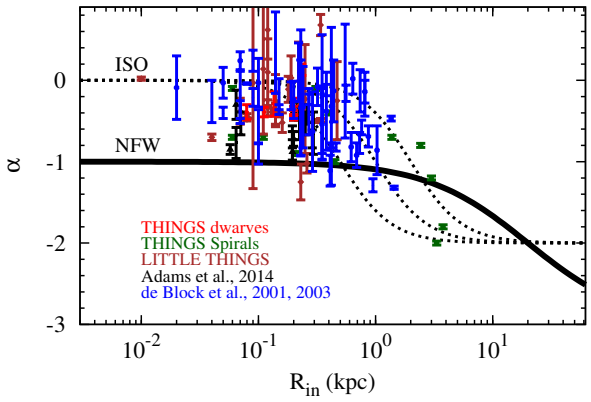


Fig. 4 Inner slope vs. $R_{\rm in}$. The last quantity, the innermost radius point, is defined by means of a least-square fit to the inner data point in the case of THINGS dwarves and LITTLE THINGS. In the Adams et al. (2014) case, $R_{\rm in}$ is obtained by adding the seeing to the fibre radius in quadrature. The solid and dashed lines represents the theoretical prediction of NFW and ISO halos. The black symbols refer to the Adams et al. (2014) data, the 7 THINGS dwarves are indicated by the red symbols visible in the figure, and the LITTLE THINGS are represented by the brown dots. The THINGS SPIRALS are shown with the green points. The **blue** symbols are the de Blok et al. (2001) data (open circles) and those of de Blok et al. (2003) are shown with triangles.

is the dynamical time, and $t_{\rm cool}$ is the cooling rate. As estimated by Nipoti and Binney (2015) (see their Sect. 3.3), this should be several tens of megayears. After star formation starts, if the clumps are destroyed by supernovae, we have to wait another $\simeq 10^7$ yr before the first star explodes.

For precision's sake, Genzel et al. (2011) observed outflows coming out from the stellar clumps parts of the clump clusters, and Genel et al. (2012) suggested that the clumps dissipate in a few tens of Myrs (Murray 2011), to 100 times this value in high-z clumps (compatible with the redshift of flattening). Moreover, Inoue and Saitoh (2011) found that clumps are even more long-lived than what found in the previous papers.

Observation of the MW favours the long life thesis of clumps. Moreover, estimates of molecular clouds lifetime is $> 10^8$ yrs (Scoville 2013). According to the previous discussion, the clumps should orbit for several dynamical times before being dissipated.

3 Results

As previously discussed, there are at least two astrophysical solutions to the cusp/core problem: a) the SNFF mechanism, and b) the DFBC mechanism. In this section, we compare the data on the slopes of galaxies spanning a range of stellar masses $M_* = 4 \times 10^6 M_\odot - 1.6 \times 10^{11} M_\odot$, with the two quoted models.

The results of the paper are presented in figures 1-5.

Figure 1 shows the inner slope in terms of the rotation velocity of the total mass. The dashed lines reproduce the α-$V_{\rm rot}$ relation calculated by Di Cintio et al. (2014) for α measured in different ranges. The red line represents the range $3 < r/\epsilon < 10$, the blue line the range $1 < r/{\rm kpc} < 2$, and the black one, the range $0.01 < r/R_{\rm vir} < 0.02$, where ϵ is the softening length, and $R_{\rm vir}$ is the virial radius. In the case of the galaxies simulated by Di Cintio et al. (2014), the red line corresponds, for the lowest mass halo to a range $0.23\ {\rm kpc} < r < 0.78\ {\rm kpc}$, and for the largest $0.94\ {\rm kpc} < r < 3.13\ {\rm kpc}$. The black line $0.60\ {\rm kpc} < r < 1.20\ {\rm kpc}$, and for the largest mass galaxy $1.30\ {\rm kpc} < r < 2.65\ {\rm kpc}$.

The black line is fitted by (see Di Cintio et al. 2014):

$$\alpha_{\rm black} = 0.132 - \log\left(\frac{\eta^{2.58}+1}{\eta^{1.99}}\right), \tag{8}$$

with

$$\eta = 0.84\left(\frac{M_*}{10^9 M_\odot}\right)^{-0.58} + 0.06\left(\frac{M_*}{10^9 M_\odot}\right)^{0.26}, \tag{9}$$

while the blue and red lines are respectively fitted by

$$\alpha_{\rm blue} = 0.167619 - \log\left[\left(10^{X+2.14248}\right)^{-0.699049} + \left(10^{X+2.14248}\right)^{1.56202}\right], \tag{10}$$

and

$$\alpha_{\rm red} = 0.230967 - \log\left[\left(10^{X+2.20929}\right)^{-0.493541} + \left(10^{X+2.20929}\right)^{1.49315}\right], \quad (11)$$

with X being

$$X = \log\left[\frac{0.0702}{\frac{10^{6.7120} M_*^{-0.57912}}{4.6570} + \frac{10^{-2.9657} M_*^{0.25589}}{0.50674}}\right]. \quad (12)$$

The equations for $\alpha_{\rm red}$ and $\alpha_{\rm blue}$ have been kindly provided by A. Di Cintio.

The previous equations give the α-dependence on M_*. In order to get the dependence on $V_{\rm rot}$, we use (Eq. 5), the stellar mass Tully-Fisher (TF) relation (Eq. 4 of Dutton et al. (2010)), similarly to Di Cintio et al. (2014). Note that the three lines in figure 6 of Di Cintio et al. (2014) and the three lines of this paper are different by a factor h inverse, coming from the Tully-Fisher relation of Dutton et al. (2010), and discarded in Di Cintio et al. (2014).

In figure 2 we compared the theoretical relations obtained by Di Cintio et al. (2014) and that obtained by means of our model with observational data. As before, the red, blue and black lines represent the slope α calculated at different distances from the galaxies centre by Di Cintio et al. (2014). The green line represents the same relation calculated with our model. They were calculated using the model in Appendix A, which is based on Del Popolo (2009) using a different recipe of gas cooling, and taking into account star formation, reionization, and supernovae feedback as described in the Appendix A (see also Del Popolo and Hiotelis 2014). The model was used to study the evolution of proto-structures and formation of structures of different masses, with final halo mass, and stellar masses similar to that studied by Di Cintio et al. (2014). For each galaxy the stellar to halo ratio was calculated, and the slope calculated in the same radial bins of Di Cintio et al. (2014) (e.g., see their figure 3). Converting the stellar mass into halo mass by means of the Moster relation (Moster et al. 2013), we can calculate the α-M_* relation. This can be converted into an α-$V_{2.2}$ relation[12], through the Tully-Fisher relation (Dutton et al. 2010, Eq. 4). Our green (yellow) line corresponds to the red (blue) one in Di Cintio et al. (2014), their figure 6. Note that the turn in the α-$V_{\rm rot}$ relation at $\simeq 25$ km/s (in the case of our model) originates from the fact that in our model the inner slope of the density profile of a structure is inversely proportional to the angular momentum (e.g. Del Popolo 2009): the larger the last the flatter is the profile. When we move from normal spiral galaxies to the dSphs region the angular momentum of the structure strongly decreases producing the steepening of the inner slope.

These models are compared with a set of data composed by the Adams et al. (2014) galaxies, the Simon et al. (2005) galaxy sample (excluding those restudied by Adams et al. 2014), the THINGS dwarves (Oh et al. 2011a,b), the THINGS galaxies (Chemin et al. 2011; Oh et al. 2015), the LITTLE THINGS galaxies, provided by Oh, and Fornax, and Sculptor, whose inner slope was calculated by Walker and Peñarrubia (2011) without adopting a DM halo model, and directly from stellar spectroscopic data. They measured the quantity $\Gamma \equiv \Delta \log M / \Delta \log r$, finding a value of $\Gamma = 2.61^{+0.43}_{-0.37}$ for Fornax, and $\Gamma = 2.95^{+0.51}_{-0.39}$ for Sculptor. The relation among Γ and α is given by $\alpha_{\rm DM} < 3 - \Gamma$ (Walker and Peñarrubia 2011). We added also a point coming from MW, obtained from the best fit to the 511 keV emission (Ascasibar et al. 2006). The figure shows that for $V_{\rm rot} > 100$ km/s, only 4 points over 9 are compatible with the theoretical models. For smaller values of the velocity, the Adams et al. (2014) galaxy sample shows a larger slope in comparison with those of other samples (as observed by the same authors). The majority of the THINGS dwarf galaxies have slope larger than the predictions. The LITTLE THINGS data can be used to constrain the models only at small velocities (< 40 km/s). They agree with the theoretical data, similarly to Sculptor and Fornax, but they have large errors. The plot shows that the main differences among the SNFF and the DFBC model are evident in the velocity range $50 - 100$ km/s. The DFBC predicts steeper slopes, with maximum differences around $\Delta\alpha \simeq 0.2$. The other difference is evident at small velocities. While the SNFF predicts slopes that steepen to cuspy, since at small velocities corresponding to $M_*/M_{\rm halo} \leq 0.01\%$ the energy from supernovae feedback is not enough to flatten the profile, the DFBC predicts flatter profiles. The reason is connected to the different mechanism the DFBC is based on. As already reported, in dSphs star formation efficiency is low. This means that if we have a fixed quantity of gas, the clumps that it forms can act directly on DM, while in the SNFF mechanism the gas must be converted into large mass stars (and as we told the efficiency is low) to explode into SNs that will inject energy in the DM.

The ability of the DFBC mechanism to form profiles flatter than the SNFF mechanism is important since it implies that dSphs of low mass are not necessarily cuspy, as predicted by the SNFF model. This means that the observation of cored profiles at small stellar masses (e.g., $< 10^6 M_\odot$) would not imply that the ΛCDM model has scarce possibilities to be correct, as it is predicted by the SNFF model (e.g., Madau et al. 2014).

In the left panel of figure 2, we plot the same quantities, except that the Adams' data are obtained from the stellar traced observations.

[12] $V_{2.2}$ is the rotation velocity for late-type galaxies, at 2.2 disc scale-lengths. $V_{2.2} \simeq V_{\rm opt}$ for the quoted late-type galaxies.

Figure 3 shows α in terms of the stellar mass M_*. The two figures give similar information as the two panels in figure 2. However, in this case we did not use Eq. 5 to transform M_* into $V_{\rm rot}$ with the result that we have smaller uncertainties. Moreover, the plots show more clearly the behaviour of the models especially at small stellar masses. The plots show that the DFBC model predicts steeper profiles in the range $10^8 M_\odot < M_* < 10^{10} M_\odot$ with respect to the SNFF model. At small stellar masses, $M_* \simeq 10^4 M_\odot$ the profile produced by the DFBC is not cuspy, at least it does not become steep as a NFW or steeper as happens to the SNFF model. Apart the visual difference among the two models, we have analysed which one describes better the data. We applied a χ^2 to the data and model (see the following subsection).

Since data having not sufficient spatial resolution can give rise to larger values of α, in cored systems, it is useful to study the behaviour of the logarithmic slope in terms of the data spatial resolution. In figure 4, we plot the logarithmic inner slope as a function of the RC's resolution. As Oh et al. (2011a), we plot data coming from THINGS dwarves, de Blok et al. (2001) (open circles), de Blok et al. (2003) (triangles). We add data from Adams et al. (2014) and the LITTLE THINGS objects. As the figure shows, at low resolution $R_{\rm in} \simeq 1$ the NFW and ISO slopes are almost equal (de Blok et al. 2001), while at high resolution, $R_{\rm in} < 1$, it is possible to distinguish the NFW and ISO slopes. The solid and dashed curves represent the theoretical NFW and ISO α-$R_{\rm in}$ relations. While the THINGS dwarves and the LITTLE THINGS deviate significantly from the NFW predictions, the Adams et al. (2014) data are somehow intermediate between the two models, namely intermediate between cuspy and cored halos.

In the following, in order to constrain the two astrophysical models able to transform cuspy profiles in cored ones, we will first use a) all the galaxies previously discussed, and then in order to get the best available distribution of slopes, and constraints on the two quoted mechanisms, we will b) include only the highest-quality results available in literature. We will then include the sets by Adams et al. (2014) and Simon et al. (2005) not re-studied in Adams et al. (2014) and some of the THINGS galaxies.

Concerning the case b, we have to choose a sample. From the previous discussions, we know that the data sets are noteworthy different. The average values of α is different for different data sets. The THINGS dwarf galaxies have $< \alpha >= -0.29 \pm 0.07$ (Oh et al. 2011b), which is significantly shallower than the Adams et al. (2014) data set having $< \alpha >= -0.67 \pm 0.10$ (stellar kinematics), and $< \alpha >= -0.58 \pm 0.024$ (gas), or those of Simon et al. (2005) with $< \alpha >= -0.73 \pm 0.44$.

The question is what originates those differences. The difference among the THINGS dwarves and the Adams et al. (2014) result could be due to the fact that the THINGS dwarves have smaller stellar masses. However, this point seems not to be so important, because the stellar mass of the THINGS dwarves is enough to give rise to a core in the quoted galaxies, according to the models of SN feedback. Oh et al. (2011b) measured the inner slopes by using a power-law fit to the innermost $\simeq 5$ points of the rotation curve ($r \simeq 1$ kpc). These points are obviously the most exposed to systematic uncertainties. The slopes measured in Adams et al. (2014) were calculated by fitting the entire density profile. Moreover, a large part of the THINGS dwarves have evident peculiarities that could bias the slopes measurement [13].

The THINGS galaxies have some drawbacks. de Blok et al. (2008) didn't derive the slopes of the THINGS galaxies as (for the spirals) these would be dominated by the stars, and corrections for them would be too uncertain. The only ones where they thought the slope would say something about the DM were the ones published in Oh et al. (2011a,b) (which are dwarves).

Other authors (Chemin et al. 2011), tried to calculate the slopes of the THINGS galaxies. They re-analysed 17 galaxies, undisturbed and rotationally dominated, in the Walter et al. (2008) sample that coincides fundamentally with that of de Blok et al. (2008) and found that the mass distributions differ from those of de Blok et al. (2008).

Also Oh et al. (2015) calculated the THINGS slopes, and the results are in many cases in conflict with those of Chemin et al. (2011). In the present paper, we use Oh et al. (2015) data for the THINGS galaxies, *for compatibility reasons*, since we also used Oh's data for THINGS dwarves and LITTLE THINGS. The reason behind it is that it is important to use galaxies whose slope is determined in a similar way and approximately at the same distance from the centre. Hence our choice for using data from Oh et al. (2015) and Adams et al. (2014) and neglecting those from Chemin et al. (2011).

This justifies the need to choose accurately the best sample from the data we have.

So, we will include the best behaved THINGS dwarves (Ho II and DDO 154), the Adams' galaxies (NGC 959; UGC 2259; NGC 2552; NGC 5204; UGC 11707) and those of Simon et al. (2005) not re-studied in Adams. This set has a $\alpha = -0.673 \pm 0.34$ almost independent of whether we use gaseous or stellar kinematics, and in strict agreement with the slopes obtained by Newman et al. (2013a) (see also Del Popolo 2014).

In figure 5, we compare the α-M_* relations with the previous sample.

[13] Holmberg I, Holmberg II, NGC 2366, DD0154, and DDO 53 have not trivial kinematic asymmetries, IC 2574, NGC 2366 have not negligible non-circular motions, and M81dwB has a rotation curve which declines.

As reported in the introduction, the cusp/core problem has been also noticed at clusters of galaxies scales. It is remarkable that the mechanism explaining the quoted observations, and the correlations found by Newman et al. (2013a,b), described in Del Popolo and Cardone (2012) and Del Popolo (2014a), is the same explaining the shallow density profiles over 6 order of magnitudes in the halo mass (dwarfs, clusters). In order to explain the galaxy clusters density profiles, Martizzi et al. (2012) had to invoke the feedback from active galactic nuclei (AGN) on the distribution of gas, finding a cores of similar size in the DM component and the stellar central component.

3.1 Determination of the best model

As shown in the previous figures, the different models do not seem, as one may expect, to reproduce the data perfectly. This is understandable since on one side the theoretical models are very approximate and suffer of many uncertainties due to the poor knowledge of the baryon physics involved, while on the other side, observational mass and inner slope determinations are affected by systematics and difficulties.

Therefore it is necessary to adopt a statistical approach to evaluate which model describes better the observations. To do so we use the χ^2 test defined as

$$\chi^2 = \sum_{k=1}^{N} \frac{(\alpha_{\rm th} - \alpha_{{\rm obs},k})^2}{\sigma_k^2} \ , \tag{13}$$

where $\alpha_{\rm th}$ and $\alpha_{\rm obs}$ are the theoretical and observed density slope respectively and σ_k^2 the error on each measurements. This test strictly requires that the error distribution is Gaussian. If this is not the case (being the error bars asymmetric), we will use the geometric mean of the two errors. Note also that we do not have any free parameter in the models, being the models dependent only on the mass of the stellar component M_* and the numerical constants determined by the underlying physical processes considered.

We will build several likelihood functions: we first consider the whole sample of data points and then the restricted subsample described in Section 3.

In a second step we will consider again all the data points, but we will apply a velocity cut-off. In particular, we will select all the points with maximum velocity $V_{\rm rot}$ smaller than 50 and 30 km/s. We do not go below this threshold since there would be not enough points. With a threshold of 50 (30) km/s we can use 27 (16) data points out of the 50 used in this work. The optimal sample is made of 10 objects.

We show our results about the reduced chi-square ($\chi^2_{\rm red}$) in table 7 using the numerical and theoretical values of the inner slope α as in figure 2. In this way we do not need any conversion from the velocity $V_{\rm rot}$ to the stellar mass M_*. Note that the values of $\chi^2_{\rm red}$ are very high, of the order of hundred per degree of freedom, due to the fact that many points lie outside the theoretical curves for many σs and the χ^2 statistics is dominated by points with very small error bars. We remind the reader that the reduced χ^2 is defined as $\chi^2_{\rm red} = \chi^2/\nu$ where ν is the number of degrees of freedom of the model.

As it appears evident, all the models perform very similarly, with marginal differences not statistically significant when we use all the data points, either with gas or stellar tracers. The situation is different when we restrict our analysis to the optimal sample. In this case the $\chi^2_{\rm red}$ for the sample containing objects whose inner slope was evaluated using stellar tracers is two times smaller than the one for the gas tracer sample. This shows the higher quality of the observations. We observe this improvement only for the optimal sample since when we apply a cut-off of 50 km/s in $V_{\rm rot}$, the two reduced χ^2 are once again very similar. It is also instructive to compare the two different models studied in this work. Comparing the models' prediction for the same range of r, we observe that when using the whole sample, the two different models behave roughly the same, with no particular preference for one or the other. Same conclusion when we consider the cut $V_{\rm rot} < 30$ km/s, with the model of this paper performing a bit better (worse) for the range $1 < r/{\rm kpc} < 2$ ($3 < r/\epsilon < 10$). When we restrict the analysis to the optimal sample, the model of this paper has a reduced $\chi^2_{\rm red}$ a factor of two smaller than the model based on the SN feedback, showing therefore a better fit to the data points.

A usual quantity that can be easily evaluated the relative probability of the models with respect to each other. This is defined as the ratio of the likelihood of the models, and in terms of the χ^2 statistics is expressed as $P(a,b) = \exp\left[-(\chi^2_a - \chi^2_b)/2\right]$ where a and b represent the two models, the SNFF and the DFBC, respectively. In other words we are asking which model is more likely to fit the data. We show our findings in table 8. As expected the values are either very small or very big, due to the fact that the χ^2 is significantly different from one. This is one more confirmation that the models fit the current data very poorly, also for the optimal sample, despite a significant improvement in terms of probability with respect to the full sample.

We can therefore conclude that while in general the two different models studied in this work perform similarly, when we restrict to a subsample of data, the model of this paper based on dynamical friction performs better than the model based on SN feedback even if not at an appreciable statistically significant level.

4 Conclusions

The aim of this work is to compare the predictions of two models thought to be able to solve the cusp/core problem

Table 7 $\chi^2_{\rm red}$ values for different samples and models.

Sample	$0.01 < r/R_{\rm vir} < 0.02$	$1 < r/{\rm kpc} < 2$	$3 < r/\epsilon < 10$	Model of this paper for $1 < r/{\rm kpc} < 2$	Model of this paper for $3 < r/\epsilon < 10$
All (gas)	139.95	144.16	153.30	128.12	150.85
All (stars)	136.71	140.88	149.15	125.81	147.61
Optimal (gas)	39.67	41.47	49.13	20.78	30.66
Optimal (stars)	21.01	22.46	25.39	8.18	12.79
$V_{\rm rot} < 50$ km/s (gas)	53.98	59.85	77.28	41.71	82.59
$V_{\rm rot} < 50$ km/s (stars)	47.20	52.96	68.74	37.28	76.30
$V_{\rm rot} < 30$ km/s	70.00	78.99	93.76	57.72	114.36

Table 8 Relative probability between the models for different samples.

Sample	$1 < r/{\rm kpc} < 2$	$3 < r/\epsilon < 10$
All (gas)	1.83×10^{-171}	7.97×10^{-27}
All (stars)	5.37×10^{-161}	4.15×10^{-17}
Optimal (gas)	3.63×10^{-41}	8.19×10^{-37}
Optimal (stars)	1.26×10^{-28}	2.33×10^{-25}
$V_{\rm rot} < 50$ km/s (gas)	3.67×10^{-103}	9.39×10^{29}
$V_{\rm rot} < 50$ km/s (stars)	2.89×10^{-89}	4.89×10^{42}
$V_{\rm rot} < 30$ km/s	5.22×10^{-70}	1.27×10^{67}

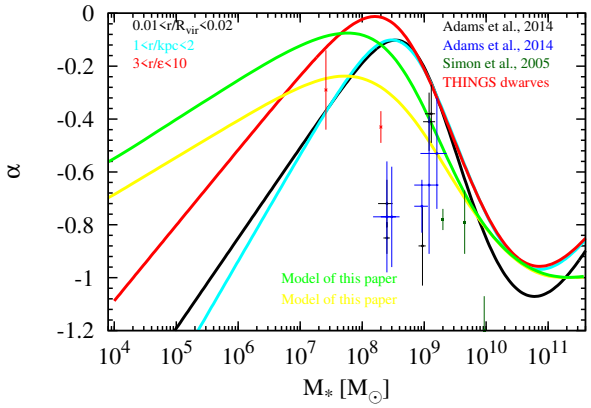


Fig. 5 Like figure 3, but now the data are only: Adams et al. (2014) galaxy sample, Simon et al. (2005) galaxies (excluding those studied by Adams et al. (2014)), and the best behaved THINGS dwarves (Ho II and DDO 154).

(Moore 1994; Flores and Primack 1994). The models taken into account are the ones based on the SN feedback (see Sect. 2.2.1) and on the baryon clumps (see Sect. 2.2.2).

The first one assumes as main driver of the flattening the internal density profile, the action of the SN explosions on the surrounding medium causing the expulsion of gas, while the second one is based on the idea that energy and angular momentum transfer from baryon clumps to the dark matter component can flatten the profile and transform a cusp into a core.

We compare the models with a sample of observational data built from different sets (see Sect. 2.1 for a detailed description). Here we limit ourselves to a short description.

One of the catalogues adopted is based on the sample of seven nearby galaxies by Adams et al. (2014) using both gas and stars as tracers, together with three additional objects studied by Simon et al. (2005). A second data set is based on seven THINGS dwarves studied by Oh et al. (2011a,b) and a third sample is based on the twenty-one objects of the LITTLE THINGS set, kindly provided by Se-Heon Oh (Oh et al. 2015). A fourth set, also provided by Se-Heon Oh (Oh et al. 2015) includes the THINGS spirals and finally, the last set is built with data for the Milky Way, Fornax and Sculptor galaxies.

Analysing figures 3 and 5 (the first with the full set of data points, the second with a restricted subsample made of the Adams et al. (2014) and Simon et al. (2005) galaxies, and the two THINGS dwarves Ho II and DDO 154) and comparing the models with a reduced chi-square $\chi^2_{\rm red}$ analysis, we see that the whole data set does not favour any of the two models in particular, while a restricted analysis to the men-

tioned higher quality subsample shows a clear preference for the model based on baryon clumps.

We also showed that dSphs of small mass ($M_* < 10^6 M_\odot$) can have cored profiles. For $M_* < 10^5 M_\odot$ the slope is $\simeq -0.6$. This is the main difference between the SNFF model and the DFBC of this paper. An important consequence is that finding a dSphs having $M_* < 10^6 M_\odot$ with an inner profile not cuspy, as predicted by the SNFF model, is not death hit for the ΛCDM model.

The last point clearly shows that the determination of the inner structure of dwarf galaxies is of fundamental importance to determine the nature of the DM. However, as already reported the inner structure of DM haloes of dSphs is still debated, since it is difficult to distinguish cuspy and cored profiles (e.g., Strigari et al. 2014). Can this problem been solved in the near future? Some authors hinted to this possibility. Future observations from the Subaru Hyper-Supreme-Camera (Takada 2010) or GAIA (de Bruijne 2012) have been indicated as a possible way out from the puzzle. In reality, even with those observations the problem will not be solved except for some larger dwarf galaxies (e.g. Sagittarius, see Richardson et al. 2014). In fact, as previously discussed, one method often used to study the density profiles is based on the Jeans equations. The method has a drawback, a degeneracy between the density profile and the anisotropy parameter β. The direct determination of this parameter is not possible having just data on the 2D projection of stars radius and from the line of sight component of stars velocity. Several improvements to the previous case have been proposed (see Battaglia et al. 2013; Richardson et al. 2014). Better results could be obtained by means of the 2+1 data sets (meaning that we know two of the three position coordinates and one of the three velocity coordinates) (see Battaglia et al. 2013). Information on the proper motions allows the determination of the density slope at half-light radius (Strigari et al. 2007). However, the proper motions of dwarf galaxy stars is challenging to determine even with GAIA (Richardson et al. 2014), with a maximum astrometric accuracy of 7 μas at magnitude $V = 10$, while it could have been possible with an error of ± 0.2, determining the proper motions of just 200 stars, with the SIM mission[14], which should have had a higher astrometric accuracy than GAIA's (Strigari et al. 2007).

Acknowledgements

The authors thank Joshua Simon and Arianna Di Cintio for useful discussions and Se-Heon Oh for kindly providing his data points.

[14]The Space Interferometry Mission, or SIM was a planned space telescope developed by USA. SIM was postponed several times and finally cancelled in 2010.

A Model

The model used in the present paper was introduced in Del Popolo (2009); Del Popolo and Hiotelis (2014), and then applied in several other papers to study the universality of the density profiles (Del Popolo 2010, 2011), the density profiles in galaxies (Del Popolo 2012a, 2014a) and clusters (Del Popolo 2012b, 2014a), and the inner surface-density of galaxies (Del Popolo et al. 2013d).

The model is a semi-analytical model (SAM) that includes an improved secondary infall model (SIM) (e.g., Gunn and Gott 1972; Hoffman and Shaham 1985; Del Popolo and Gambera 1997; Ascasibar et al. 2004; Williams et al. 2004; Hiotelis and Del Popolo 2006, 2013; Cardone et al. 2011a; Del Popolo et al. 2013b,c). Differently from previous SIMs, the model considers the effects of non-radial collapse originated by random angular momentum [15], adiabatic contraction of DM that baryons produce (Blumenthal et al. 1986; Gnedin et al. 2004; Gustafsson et al. 2006), dynamical friction effects (e.g., El-Zant et al. 2001, 2004), random and ordered angular momentum. The model takes into account reionization, cooling, star formation, and the supernova feedback (see the following).

The model follows the evolution of a perturbation starting from the linear phase, expanding with the Hubble flow till the phase of maximum expansion (turn-around). In the following phases of collapse and "shell-crossing", it is assumed that the central potential varies adiabatically (Gunn 1977; Fillmore and Goldreich 1984). The final profile is given by

$$\rho(x)=\frac{\rho_{\rm ta}(x_{\rm m})}{f(x_{\rm i})^3}\left[1+\frac{d\ln f(x_{\rm i})}{d\ln g(x_{\rm i})}\right]^{-1}\ , \tag{A1}$$

where we indicated the initial radius with $x_{\rm i}$, the collapse factor with $f(x_{\rm i})=x/x_{\rm m}(x_{\rm i})$, and the turn-around radius with $x_{\rm m}(x_{\rm i})$, given by

$$x_{\rm m}=g(x_{\rm i})=x_{\rm i}\frac{1+\overline{\delta}_{\rm i}}{\overline{\delta}_{\rm i}-(\Omega_{\rm i}^{-1}-1)}\ . \tag{A2}$$

In the previous equation, $\Omega_{\rm i}$ is the density parameter, and $\overline{\delta}_{\rm i}$ the average overdensity in a given shell. Our model contains DM and baryons. Initially, baryons are in the gas phase. Baryon fraction is set equal to the "universal baryon fraction" $f_{\rm b}=0.17\pm0.01$ (Komatsu et al. 2009) (0.167 in Komatsu et al. 2011). The baryonic fraction is obtained from the star formation processes described in the following.

In the model, the "ordered angular momentum" h (coming from tidal torques of large scale structures on those on the smaller scales) is obtained through the tidal torque theory (TTT) (Hoyle 1953; Peebles 1969; White 1984; Ryden 1988; Eisenstein and Loeb 1995). The "random angular momentum" j is expressed in terms of the eccentricity $e=\left(\frac{r_{\rm min}}{r_{\rm max}}\right)$ (Avila-Reese et al. 1998), where $r_{\rm max}$ is the apocentric radius, and $r_{\rm min}$ the pericentric radius. A correction on the eccentricity is made, according to simulations of Ascasibar et al. (2004), which consider the effects of the dynamical state of the system on eccentricity

$$e(r_{\rm max})\simeq 0.8\left(\frac{r_{\rm max}}{r_{\rm ta}}\right)^{0.1}\ , \tag{A3}$$

for $r_{\rm max}<0.1r_{\rm ta}$.

The steepening of the profile produced by the adiabatic compression was obtained following Gnedin et al. (2004), and calculated using iterative techniques Spedicato et al. (2003), while the effects of dynamical friction were obtained adding the dynamical friction force, calculated as described in Appendix A of Del Popolo (2009), to the equation of motions (see Del Popolo 2009, Eq. A14).

Gas cooling, star formation, reionization and supernovae feedback were included as done by De Lucia and Helmi (2008) and Li et al. (2010) (Sect. 2.2.2 and 2.2.3).

Reionization, treated as in Li et al. (2010), reduces the baryon content, and the baryon fraction changes as

$$f_{\rm b,halo}(z,M_{\rm vir})=\frac{f_{\rm b}}{[1+0.26M_{\rm F}(z)/M_{\rm vir}]^3}\ , \tag{A4}$$

where $M_{\rm F}$, is the "filtering mass" (see Kravtsov et al. 2004), and as usual the virial mass is indicated as $M_{\rm vir}$. The reionization redshift is in the range 11.5-15.

[15] The random angular momentum arises from the system random velocities (Ryden and Gunn 1987).

Gas cooling is treated as a classical cooling flow (e.g., White and Frenk 1991) (see Sect. 2.2.2 of Li et al. 2010). Similar results are obtained using the Ryden (1988) treatment.

The details of star formation are given in De Lucia and Helmi (2008). The treatment of Croton et al. (2006) is used for the supernovae feedback. In Di Cintio et al. (2014) it was used the blast wave SN feedback (Stinson et al. 2006). For our purposes, the choice of the formalism, even if similar, is not so fundamental. A fundamental difference among our model and the SNFF model (e.g., Di Cintio et al. 2014) is that in our case the flattening process happens before star formation, and the source of energy is gravitational. Stellar feedback acts when the core is already formed, and disrupts the gas clouds. In the SNFF model the flattening process happens after star formation and the source of energy is stellar feedback.

Concerning these last steps. Gas forms a disc, and the star formation rate is

$$\psi = 0.03 M_{\rm sf}/t_{\rm dyn} \ , \tag{A5}$$

being $t_{\rm dyn}$ the disc dynamical time, and $M_{\rm sf}$ the gas mass above a given density threshold, $n > 9.3/cm^3$ as in Di Cintio et al. (2014). The initial mass function (IMF) is a Chabrier one (Chabrier 2003). The amount of stars forming is given by

$$\Delta M_* = \psi \Delta t \ , \tag{A6}$$

where Δt indicates the time-step.

The quantity of energy injected by SN in the ISM is

$$\Delta E_{\rm SN} = 0.5 \epsilon_{\rm halo} \Delta M_* V_{\rm SN}^2 \ , \tag{A7}$$

where $V_{\rm SN}^2 = \eta_{\rm SN} E_{\rm SN}$ is the energy injected per supernovae and per unit solar mass. The efficiency reheating disc gas efficiency produced by energy is fixed at $\epsilon_{\rm halo} = 0.35$ (Li et al. 2010). $\eta_{\rm SN} = 8 \times 10^{-3}/M_\odot$ gives the supernovae number per solar mass obtained assuming a Chabrier IMF (Chabrier 2003), and the typical energy released in a SN explosion is $E_{\rm SN} = 10^{51}$ erg.

Energy injection in the gas reheats it proportionally to the number of star formed

$$\Delta M_{\rm reheat} = 3.5 \Delta M_* \ . \tag{A8}$$

The change in thermal energy produced by the reheated gas is given by

$$\Delta E_{\rm hot} = 0.5 \Delta M_{\rm reheat} V_{\rm vir}^2 \ , \tag{A9}$$

This hot gas will be ejected by the halo if $\Delta E_{\rm SN} > \Delta E_{\rm hot}$, and the quantity is

$$\Delta M_{\rm eject} = \frac{\Delta E_{\rm SN} - \Delta E_{\rm hot}}{0.5 V_{\rm vir}^2} \ . \tag{A10}$$

The halo can accrete the ejected material that becomes part of the hot component related to the central galaxy (De Lucia et al. 2004; Croton et al. 2006).

The results of the previous model are in agreement with previous studies on the cusp flattening produced by heating of DM by collapsing clumps of baryons (El-Zant et al. 2001, 2004; Romano-Díaz et al. 2008; Cole et al. 2011; Inoue and Saitoh 2011; Nipoti and Binney 2015), and as previously reported predicted the correct shape of galaxy, and clusters density profiles together with a series of correlations found in observations like those of Newman et al. (2013a,b).

References

Adams, J.J., Gebhardt, K., Blanc, G.A., Fabricius, M.H., Hill, G.J., Murphy, J.D., van den Bosch, R.C.E., van de Ven, G.: ApJ **745**, 92 (2012). 1110.5951. doi:10.1088/0004-637X/745/1/92

Adams, J.J., Simon, J.D., Fabricius, M.H., van den Bosch, R.C.E., Barentine, J.C., Bender, R., Gebhardt, K., Hill, G.J., Murphy, J.D., Swaters, R.A., Thomas, J., van de Ven, G.: ApJ **789**, 63 (2014). 1405.4854. doi:10.1088/0004-637X/789/1/63

Agertz, O., Teyssier, R., Moore, B.: MNRAS **397**, 64 (2009). 0901.2536. doi:10.1111/j.1745-3933.2009.00685.x

Agnello, A., Evans, N.W.: ApJL **754**, 39 (2012). 1205.6673. doi:10.1088/2041-8205/754/2/L39

Amorisco, N.C., Evans, N.W.: MNRAS **419**, 184 (2012). 1106.1062. doi:10.1111/j.1365-2966.2011.19684.x

Ascasibar, Y., Yepes, G., Gottlöber, S., Müller, V.: MNRAS **352**, 1109 (2004). arXiv:astro-ph/0312221. doi:10.1111/j.1365-2966.2004.08005.x

Ascasibar, Y., Jean, P., Bœhm, C., Knödlseder, J.: MNRAS **368**, 1695 (2006). astro-ph/0507142. doi:10.1111/j.1365-2966.2006.10226.x

Astashenok, A.V., del Popolo, A.: Classical and Quantum Gravity **29**(8), 085014 (2012). 1203.2290. doi:10.1088/0264-9381/29/8/085014

Avila-Reese, V., Firmani, C., Hernández, X.: ApJ **505**, 37 (1998). astro-ph/9710201. doi:10.1086/306136

Barnabè, M., Dutton, A.A., Marshall, P.J., Auger, M.W., Brewer, B.J., Treu, T., Bolton, A.S., Koo, D.C., Koopmans, L.V.E.: MNRAS **423**, 1073 (2012). 1201.1692. doi:10.1111/j.1365-2966.2012.20934.x

Battaglia, G., Helmi, A., Breddels, M.: New Astronomy Reviews **57**, 52 (2013). 1305.5965. doi:10.1016/j.newar.2013.05.003

Battaglia, G., Helmi, A., Tolstoy, E., Irwin, M., Hill, V., Jablonka, P.: ApJL **681**, 13 (2008). 0802.4220. doi:10.1086/590179

Bengochea, G.R., Ferraro, R.: Phys. Rev. D **79**(12), 124019 (2009). 0812.1205. doi:10.1103/PhysRevD.79.124019

Blumenthal, G.R., Faber, S.M., Flores, R., Primack, J.R.: ApJ **301**, 27 (1986). doi:10.1086/163867

Bournaud, F., Elmegreen, B.G., Martig, M.: ApJL **707**, 1 (2009). 0910.3677. doi:10.1088/0004-637X/707/1/L1

Bournaud, F., Perret, V., Renaud, F., Dekel, A., Elmegreen, B.G., Elmegreen, D.M., Teyssier, R., Amram, P., Daddi, E., Duc, P.-A., Elbaz, D., Epinat, B., Gabor, J.M., Juneau, S., Kraljic, K., Le Floch', E.: ApJ **780**, 57 (2014). 1307.7136. doi:10.1088/0004-637X/780/1/57

Bovill, M.S., Ricotti, M.: ApJ **741**, 17 (2011a). 1010.2231. doi:10.1088/0004-637X/741/1/17

Bovill, M.S., Ricotti, M.: ApJ **741**, 18 (2011b). 1010.2233. doi:10.1088/0004-637X/741/1/18

Boylan-Kolchin, M., Bullock, J.S., Kaplinghat, M.: MNRAS **415**, 40 (2011). 1103.0007. doi:10.1111/j.1745-3933.2011.01074.x

Boylan-Kolchin, M., Bullock, J.S., Kaplinghat, M.: MNRAS **422**, 1203 (2012). 1111.2048. doi:10.1111/j.1365-2966.2012.20695.x

Breddels, M.A., Helmi, A., van den Bosch, R.C.E., van de Ven, G., Battaglia, G.: MNRAS **433**, 3173 (2013). 1205.4712. doi:10.1093/mnras/stt956

Brook, C.B., Di Cintio, A.: ArXiv e-prints (2014). 1410.3825

Buchdahl, H.A.: MNRAS **150**, 1 (1970)

Burkert, A.: ApJL **447**, 25 (1995). astro-ph/9504041. doi:10.1086/309560

Cappellari, M.: MNRAS **390**, 71 (2008). 0806.0042. doi:10.1111/j.1365-2966.2008.13754.x

Cardone, V.F., Del Popolo, A.: MNRAS **427**, 3176 (2012). 1209.1524. doi:10.1111/j.1365-2966.2012.21982.x

Cardone, V.F., Leubner, M.P., Del Popolo, A.: MNRAS **414**, 2265 (2011a). 1102.3319. doi:10.1111/j.1365-2966.2011.18543.x

Cardone, V.F., Del Popolo, A., Tortora, C., Napolitano, N.R.: MNRAS **416**, 1822 (2011b). 1106.0364. doi:10.1111/j.1365-2966.2011.19162.x

Ceverino, D., Dekel, A., Bournaud, F.: MNRAS **404**, 2151 (2010). 0907.3271. doi:10.1111/j.1365-2966.2010.16433.x

Chabrier, G.: PASP **115**, 763 (2003). astro-ph/0304382. doi:10.1086/376392

Chemin, L., de Blok, W.J.G., Mamon, G.A.: AJ **142**, 109 (2011). 1109.4247. doi:10.1088/0004-6256/142/4/109

Choi, E., Ostriker, J.P., Naab, T., Oser, L., Moster, B.P.: ArXiv e-prints, 1403.1257 (2014). 1403.1257

Cole, D.R., Dehnen, W., Wilkinson, M.I.: MNRAS **416**, 1118 (2011). 1105.4050. doi:10.1111/j.1365-2966.2011.19110.x

Colín, P., Avila-Reese, V., Valenzuela, O.: ApJ **542**, 622 (2000). astro-ph/0004115. doi:10.1086/317057

Croton, D.J., Springel, V., White, S.D.M., De Lucia, G., Frenk, C.S., Gao, L., Jenkins, A., Kauffmann, G., Navarro, J.F., Yoshida, N.: MNRAS **365**, 11 (2006). astro-ph/0508046. doi:10.1111/j.1365-2966.2005.09675.x

de Blok, W.J.G., McGaugh, S.S.: MNRAS **290**, 533 (1997). astro-ph/9704274

de Blok, W.J.G., Bosma, A., McGaugh, S.: MNRAS **340**, 657 (2003). astro-ph/0212102. doi:10.1046/j.1365-8711.2003.06330.x

de Blok, W.J.G., McGaugh, S.S., Bosma, A., Rubin, V.C.: ApJL **552**, 23 (2001). astro-ph/0103102. doi:10.1086/320262

de Blok, W.J.G., Walter, F., Brinks, E., Trachternach, C., Oh, S.-H., Kennicutt, R.C. Jr.: AJ **136**, 2648 (2008). 0810.2100. doi:10.1088/0004-6256/136/6/2648

de Boer, T.J.L., Tolstoy, E., Hill, V., Saha, A., Olszewski, E.W., Mateo, M., Starkenburg, E., Battaglia, G., Walker, M.G.: A&A **544**, 73 (2012a). 1206.6968. doi:10.1051/0004-6361/201219547

de Boer, T.J.L., Tolstoy, E., Hill, V., Saha, A., Olsen, K., Starkenburg, E., Lemasle, B., Irwin, M.J., Battaglia, G.: A&A **539**, 103 (2012b). 1201.2408. doi:10.1051/0004-6361/201118378

de Bruijne, J.H.J.: Ap&SS **341**, 31 (2012). 1201.3238. doi:10.1007/s10509-012-1019-4

De Lucia, G., Helmi, A.: MNRAS **391**, 14 (2008). 0804.2465. doi:10.1111/j.1365-2966.2008.13862.x

De Lucia, G., Kauffmann, G., White, S.D.M.: MNRAS **349**, 1101 (2004). astro-ph/0310268. doi:10.1111/j.1365-2966.2004.07584.x

Del Popolo, A.: MNRAS **336**, 81 (2002). astro-ph/0205449. doi:10.1046/j.1365-8711.2002.05697.x

Del Popolo, A.: Astronomy Reports **51**, 169 (2007). 0801.1091. doi:10.1134/S1063772907030018

Del Popolo, A.: ApJ **698**, 2093 (2009). 0906.4447. doi:10.1088/0004-637X/698/2/2093

Del Popolo, A.: MNRAS **408**, 1808 (2010). 1012.4322. doi:10.1111/j.1365-2966.2010.17288.x
Del Popolo, A.: JCAP **7**, 14 (2011). 1112.4185. doi:10.1088/1475-7516/2011/07/014
Del Popolo, A.: MNRAS **419**, 971 (2012a). 1105.0090. doi:10.1111/j.1365-2966.2011.19754.x
Del Popolo, A.: MNRAS **424**, 38 (2012b). 1204.4439. doi:10.1111/j.1365-2966.2012.21141.x
Del Popolo, A.: In: AIP Conf. Proc., vol. 1548, p. 2 (2013). doi:10.1063/1.4817029
Del Popolo, A.: International Journal of Modern Physics D **23**, 30005 (2014a). 1305.0456. doi:10.1142/S0218271814300055
Del Popolo, A.: JCAP **7**, 19 (2014b). 1407.4347. doi:10.1088/1475-7516/2014/07/019
Del Popolo, A., Cardone, V.F.: MNRAS **423**, 1060 (2012). 1203.3377. doi:10.1111/j.1365-2966.2012.20936.x
Del Popolo, A., Gambera, M.: A&A **308**, 373 (1996)
Del Popolo, A., Gambera, M.: A&A **321**, 691 (1997). astro-ph/9610052
Del Popolo, A., Gambera, M.: A&A **357**, 809 (2000). astro-ph/9909156
Del Popolo, A., Hiotelis, N.: JCAP **1**, 47 (2014). 1401.6577. doi:10.1088/1475-7516/2014/01/047
Del Popolo, A., Kroupa, P.: A&A **502**, 733 (2009). 0906.1146. doi:10.1051/0004-6361/200811404
Del Popolo, A., Le Delliou, M.: JCAP **12**, 51 (2014). 1408.4893. doi:10.1088/1475-7516/2014/12/051
Del Popolo, A., Cardone, V.F., Belvedere, G.: MNRAS **429**, 1080 (2013a). 1212.6797. doi:10.1093/mnras/sts389
Del Popolo, A., Pace, F., Lima, J.A.S.: International Journal of Modern Physics D **22**, 50038 (2013b). 1207.5789. doi:10.1142/S0218271813500387
Del Popolo, A., Pace, F., Lima, J.A.S.: MNRAS **430**, 628 (2013c). 1212.5092. doi:10.1093/mnras/sts669
Del Popolo, A., Pace, F., Maydanyuk, S.P., Lima, J.A.S., Jesus, J.F.: Phys. Rev. D 87(4), 043527 (2013d). arxivurl1303.3628. doi:10.1103/PhysRevD.87.043527
Del Popolo, A., Lima, J.A.S., Fabris, J.C., Rodrigues, D.C.: JCAP **4**, 21 (2014). 1404.3674. doi:10.1088/1475-7516/2014/04/021
Dent, J.B., Dutta, S., Saridakis, E.N.: JCAP **1**, 9 (2011). 1010.2215. doi:10.1088/1475-7516/2011/01/009
Di Cintio, A., Brook, C.B., Macciò, A.V., Stinson, G.S., Knebe, A., Dutton, A.A., Wadsley, J.: MNRAS **437**, 415 (2014). 1306.0898. doi:10.1093/mnras/stt1891
Donato, F., Gentile, G., Salucci, P.: MNRAS **353**, 17 (2004). astro-ph/0403206. doi:10.1111/j.1365-2966.2004.08220.x
Dutton, A.A., Conroy, C., van den Bosch, F.C., Prada, F., More, S.: MNRAS **407**, 2 (2010). 1004.4626. doi:10.1111/j.1365-2966.2010.16911.x
Eisenstein, D.J., Loeb, A.: ApJ **439**, 520 (1995). arXiv:astro-ph/9405012. doi:10.1086/175193
El-Zant, A., Shlosman, I., Hoffman, Y.: ApJ **560**, 636 (2001). astro-ph/0103386. doi:10.1086/322516
El-Zant, A.A., Hoffman, Y., Primack, J., Combes, F., Shlosman, I.: ApJL **607**, 75 (2004). astro-ph/0309412. doi:10.1086/421938
Elmegreen, D.M., Elmegreen, B.G., Hirst, A.C.: ApJL **604**, 21 (2004). astro-ph/0402477. doi:10.1086/383312
Elmegreen, D.M., Elmegreen, B.G., Marcus, M.T., Shahinyan, K., Yau, A., Petersen, M.: ApJ **701**, 306 (2009). 0906.2660. doi:10.1088/0004-637X/701/1/306
Evans, N.W., An, J., Walker, M.G.: MNRAS **393**, 50 (2009). 0811.1488. doi:10.1111/j.1745-3933.2008.00596.x
Ferrero, I., Abadi, M.G., Navarro, J.F., Sales, L.V., Gurovich, S.: MNRAS **425**, 2817 (2012). 1111.6609. doi:10.1111/j.1365-2966.2012.21623.x
Fillmore, J.A., Goldreich, P.: ApJ **281**, 1 (1984). doi:10.1086/162070
Flores, R.A., Primack, J.R.: ApJL **427**, 1 (1994). astro-ph/9402004. doi:10.1086/187350
Fukushige, T., Makino, J.: ApJ **557**, 533 (2001). astro-ph/0008104. doi:10.1086/321666
Gao, L., Navarro, J.F., Cole, S., Frenk, C.S., White, S.D.M., Springel, V., Jenkins, A., Neto, A.F.: MNRAS **387**, 536 (2008). 0711.0746. doi:10.1111/j.1365-2966.2008.13277.x
Garrison-Kimmel, S., Rocha, M., Boylan-Kolchin, M., Bullock, J.S., Lally, J.: MNRAS **433**, 3539 (2013). 1301.3137. doi:10.1093/mnras/stt984
Garrison-Kimmel, S., Boylan-Kolchin, M., Bullock, J.S., Kirby, E.N.: MNRAS **444**, 222 (2014). 1404.5313. doi:10.1093/mnras/stu1477
Gelato, S., Sommer-Larsen, J.: MNRAS **303**, 321 (1999). astro-ph/9806289. doi:10.1046/j.1365-8711.1999.02223.x
Genel, S., Naab, T., Genzel, R., Förster Schreiber, N.M., Sternberg, A., Oser, L., Johansson, P.H., Davé, R., Oppenheimer, B.D., Burkert, A.: ApJ **745**, 11 (2012). 1011.0433. doi:10.1088/0004-637X/745/1/11
Genzel, R., Newman, S., Jones, T., Förster Schreiber, N.M., Shapiro, K., Genel, S., Lilly, S.J., et al.: ApJ **733**, 101 (2011). 1011.5360. doi:10.1088/0004-637X/733/2/101
Gnedin, O.Y., Zhao, H.: MNRAS **333**, 299 (2002). astro-ph/0108108. doi:10.1046/j.1365-8711.2002.05361.x
Gnedin, O.Y., Kravtsov, A.V., Klypin, A.A., Nagai, D.: ApJ **616**, 16 (2004). astro-ph/0406247. doi:10.1086/424914
Goodman, J.: New Astronomy **5**, 103 (2000). astro-ph/0003018. doi:10.1016/S1384-1076(00)00015-4
Governato, F., Brook, C., Mayer, L., Brooks, A., Rhee, G., Wadsley, J., Jonsson, P., Willman, B., Stinson, G., Quinn, T., Madau, P.: Nature **463**, 203 (2010). 0911.2237. doi:10.1038/nature08640
Governato, F., Zolotov, A., Pontzen, A., Christensen, C., Oh, S.H., Brooks, A.M., Quinn, T., Shen, S., Wadsley, J.: MNRAS **422**, 1231 (2012). 1202.0554. doi:10.1111/j.1365-2966.2012.20696.x
Gunn, J.E.: ApJ **218**, 592 (1977). doi:10.1086/155715
Gunn, J.E., Gott, J.R. III: ApJ **176**, 1 (1972). doi:10.1086/151605
Gustafsson, M., Fairbairn, M., Sommer-Larsen, J.: Phys. Rev. D **74**(12), 123522 (2006). astro-ph/0608634. doi:10.1103/PhysRevD.74.123522
Hayashi, K., Chiba, M.: ApJ **755**, 145 (2012). 1206.3888. doi:10.1088/0004-637X/755/2/145

Hinshaw, G., Larson, D., Komatsu, E., Spergel, D.N., Bennett, C.L., Dunkley, J., Nolta, M.R., Halpern, M., Hill, R.S., eet al.: ApJS **208**, 19 (2013). 1212.5226. doi:10.1088/0067-0049/208/2/19
Hiotelis, N., Del Popolo, A.: Ap&SS **301**, 167 (2006). astro-ph/0508531. doi:10.1007/s10509-006-1381-1
Hiotelis, N., Del Popolo, A.: Mon. Not. R. Astron. Soc. 436, 163 (2013). doi:10.1093/mnras/stt1556
Hoffman, Y., Shaham, J.: ApJ **297**, 16 (1985). doi:10.1086/163498
Hopkins, P.F., Quataert, E., Murray, N.: MNRAS **421**, 3488 (2012). 1110.4636. doi:10.1111/j.1365-2966.2012.20578.x
Hoyle, F.: ApJ **118**, 513 (1953). doi:10.1086/145780
Hu, W., Barkana, R., Gruzinov, A.: Physical Review Letters **85**, 1158 (2000). astro-ph/0003365. doi:10.1103/PhysRevLett.85.1158
Inoue, S., Saitoh, T.R.: MNRAS **418**, 2527 (2011). 1108.0906. doi:10.1111/j.1365-2966.2011.19873.x
Jardel, J.R., Gebhardt, K.: ApJ **746**, 89 (2012). 1112.0319. doi:10.1088/0004-637X/746/1/89
Jardel, J.R., Gebhardt, K.: ApJL **775**, 30 (2013). doi:10.1088/2041-8205/775/1/L30
Jardel, J.R., Gebhardt, K., Fabricius, M.H., Drory, N., Williams, M.J.: ApJ **763**, 91 (2013). 1211.5376. doi:10.1088/0004-637X/763/2/91
Jing, Y.P., Suto, Y.: ApJL **529**, 69 (2000). astro-ph/9909478. doi:10.1086/312463
Kaplinghat, M., Knox, L., Turner, M.S.: Physical Review Letters **85**, 3335 (2000). astro-ph/0005210. doi:10.1103/PhysRevLett.85.3335
Katz, N., White, S.D.M.: ApJ **412**, 455 (1993). doi:10.1086/172935
Kennicutt, R.C. Jr., Armus, L., Bendo, G., Calzetti, D., Dale, D.A., Draine, B.T., Engelbracht, C.W., et al.: PASP **115**, 928 (2003). astro-ph/0305437. doi:10.1086/376941
Komatsu, E., Dunkley, J., Nolta, M.R., *et al.*: ApJS **180**, 330 (2009). 0803.0547. doi:10.1088/0067-0049/180/2/330
Komatsu, E., Smith, K.M., Dunkley, J., et al.: ApJS **192**, 18 (2011). 1001.4538. doi:10.1088/0067-0049/192/2/18
Kravtsov, A.V., Gnedin, O.Y., Klypin, A.A.: ApJ **609**, 482 (2004). astro-ph/0401088. doi:10.1086/421322
Kuzio de Naray, R., Kaufmann, T.: MNRAS **414**, 3617 (2011). 1012.3471. doi:10.1111/j.1365-2966.2011.18656.x
Laporte, C.F.P., Peñarrubia, J.: MNRAS **449**, 90 (2015). 1409.3848. doi:10.1093/mnrasl/slv008
Laporte, C.F.P., White, S.D.M.: MNRAS **451**, 1177 (2015). 1409.1924. doi:10.1093/mnras/stv112
Li, Y.-S., De Lucia, G., Helmi, A.: MNRAS **401**, 2036 (2010). 0909.1291. doi:10.1111/j.1365-2966.2009.15803.x
Linder, E.V.: Phys. Rev. D **81**(12), 127301 (2010). 1005.3039. doi:10.1103/PhysRevD.81.127301
Ma, C.-P., Boylan-Kolchin, M.: Physical Review Letters **93**(2), 021301 (2004). astro-ph/0403102. doi:10.1103/PhysRevLett.93.021301
Madau, P., Shen, S., Governato, F.: ApJL **789**, 17 (2014). 1405.2577. doi:10.1088/2041-8205/789/1/L17
Marinacci, F., Pakmor, R., Springel, V.: MNRAS **437**, 1750 (2014). 1305.5360. doi:10.1093/mnras/stt2003
Martinsson, T.P.K., Verheijen, M.A.W., Westfall, K.B., Bershady, M.A., Andersen, D.R., Swaters, R.A.: A&A **557**, 131 (2013). 1308.0336. doi:10.1051/0004-6361/201321390
Martizzi, D., Teyssier, R., Moore, B., Wentz, T.: MNRAS **422**, 3081 (2012). 1112.2752. doi:10.1111/j.1365-2966.2012.20879.x
Mashchenko, S., Couchman, H.M.P., Sills, A.: ApJ **639**, 633 (2006). astro-ph/0511361. doi:10.1086/499582
Mashchenko, S., Wadsley, J., Couchman, H.M.P.: Science **319**, 174 (2008). 0711.4803. doi:10.1126/science.1148666
McGaugh, S.S., de Blok, W.J.G., Schombert, J.M., Kuzio de Naray, R., Kim, J.H.: ApJ **659**, 149 (2007). astro-ph/0612410. doi:10.1086/511807
Milgrom, M.: ApJ **270**, 371 (1983a). doi:10.1086/161131
Milgrom, M.: ApJ **270**, 365 (1983b). doi:10.1086/161130
Moore, B.: Nature **370**, 629 (1994). doi:10.1038/370629a0
Moore, B., Governato, F., Quinn, T., Stadel, J., Lake, G.: ApJL **499**, 5 (1998). astro-ph/9709051. doi:10.1086/311333
Moore, B., Quinn, T., Governato, F., Stadel, J., Lake, G.: MNRAS **310**, 1147 (1999). astro-ph/9903164. doi:10.1046/j.1365-8711.1999.03039.x
Moster, B.P., Naab, T., White, S.D.M.: MNRAS **428**, 3121 (2013). 1205.5807. doi:10.1093/mnras/sts261
Murray, N.: ApJ **729**, 133 (2011). 1007.3270. doi:10.1088/0004-637X/729/2/133
Murray, N., Quataert, E., Thompson, T.A.: ApJ **709**, 191 (2010). 0906.5358. doi:10.1088/0004-637X/709/1/191
Navarro, J.F., Eke, V.R., Frenk, C.S.: MNRAS **283**, 72 (1996a). astro-ph/9610187
Navarro, J.F., Frenk, C.S., White, S.D.M.: ApJ **462**, 563 (1996b). astro-ph/9508025. doi:10.1086/177173
Navarro, J.F., Frenk, C.S., White, S.D.M.: ApJ **490**, 493 (1997). astro-ph/9611107. doi:10.1086/304888
Navarro, J.F., Ludlow, A., Springel, V., Wang, J., Vogelsberger, M., White, S.D.M., Jenkins, A., Frenk, C.S., Helmi, A.: MNRAS **402**, 21 (2010). 0810.1522. doi:10.1111/j.1365-2966.2009.15878.x
Newman, A.B., Treu, T., Ellis, R.S., Sand, D.J., Nipoti, C., Richard, J., Jullo, E.: ApJ **765**, 24 (2013a). 1209.1391. doi:10.1088/0004-637X/765/1/24
Newman, A.B., Treu, T., Ellis, R.S., Sand, D.J.: ApJ **765**, 25 (2013b). 1209.1392. doi:10.1088/0004-637X/765/1/25
Nipoti, C., Binney, J.: MNRAS **446**, 1820 (2015). 1410.6169. doi:10.1093/mnras/stu2217
Nipoti, C., Treu, T., Ciotti, L., Stiavelli, M.: MNRAS **355**, 1119 (2004). astro-ph/0404127. doi:10.1111/j.1365-2966.2004.08385.x
Noguchi, M.: Nature **392**, 253 (1998). doi:10.1038/32596
Noguchi, M.: ApJ **514**, 77 (1999). astro-ph/9806355. doi:10.1086/306932
Oh, S.-H., de Blok, W.J.G., Walter, F., Brinks, E., Kennicutt, R.C. Jr.: AJ **136**, 2761 (2008). 0810.2119. doi:10.1088/0004-6256/136/6/2761

Oh, S.-H., de Blok, W.J.G., Brinks, E., Walter, F., Kennicutt, R.C. Jr.: AJ **141**, 193 (2011a). 1011.0899. doi:10.1088/0004-6256/141/6/193
Oh, S.-H., Brook, C., Governato, F., Brinks, E., Mayer, L., de Blok, W.J.G., Brooks, A., Walter, F.: AJ **142**, 24 (2011b). 1011.2777. doi:10.1088/0004-6256/142/1/24
Oh, S.-H., Hunter, D.A., Brinks, E., Elmegreen, B.G., Schruba, A., Walter, F., Rupen, M.P., Young, L.M., Simpson, C.E., Johnson, M.C., Herrmann, K.A., Ficut-Vicas, D., Cigan, P., Heesen, V., Ashley, T., Zhang, H.-X.: AJ **149**, 180 (2015). 1502.01281. doi:10.1088/0004-6256/149/6/180
Oman, K.A., Navarro, J.F., Fattahi, A., Frenk, C.S., Sawala, T., White, S.D.M., Bower, R., Crain, R.A., Furlong, M., Schaller, M., Schaye, J., Theuns, T.: MNRAS **452**, 3650 (2015). 1504.01437. doi:10.1093/mnras/stv1504
Oman, K.A., Navarro, J.F., Sales, L.V., Fattahi, A., Frenk, C.S., Sawala, T., Schaller, M., White, S.D.M.: ArXiv e-prints (2016). 1601.01026
Papastergis, E., Giovanelli, R., Haynes, M.P., Shankar, F.: A&A **574**, 113 (2015). 1407.4665. doi:10.1051/0004-6361/201424909
Peñarrubia, J., Pontzen, A., Walker, M.G., Koposov, S.E.: ApJL **759**, 42 (2012). 1207.2772. doi:10.1088/2041-8205/759/2/L42
Peebles, P.J.E.: ApJ **155**, 393 (1969). doi:10.1086/149876
Peebles, P.J.E.: ApJL **534**, 127 (2000). astro-ph/0002495. doi:10.1086/312677
Planck Collaboration XVI: A&A **571**, 16 (2014). 1303.5076. doi:10.1051/0004-6361/201321591
Polisensky, E., Ricotti, M.: MNRAS **437**, 2922 (2014). 1310.0430. doi:10.1093/mnras/stt2105
Polisensky, E., Ricotti, M.: MNRAS **450**, 2172 (2015). 1504.02126. doi:10.1093/mnras/stv736
Pontzen, A., Governato, F.: MNRAS **421**, 3464 (2012). 1106.0499. doi:10.1111/j.1365-2966.2012.20571.x
Read, J.I., Gilmore, G.: MNRAS **356**, 107 (2005). astro-ph/0409565. doi:10.1111/j.1365-2966.2004.08424.x
Revaz, Y., Jablonka, P.: A&A **538**, 82 (2012). 1109.0989. doi:10.1051/0004-6361/201117402
Richardson, T., Fairbairn, M.: MNRAS **432**, 3361 (2013). 1207.1709. doi:10.1093/mnras/stt686
Richardson, T.D., Spolyar, D., Lehnert, M.D.: MNRAS **440**, 1680 (2014). 1311.1522. doi:10.1093/mnras/stu383
Ricotti, M.: MNRAS **344**, 1237 (2003). astro-ph/0212146. doi:10.1046/j.1365-8711.2003.06910.x
Ricotti, M., Wilkinson, M.I.: MNRAS **353**, 867 (2004). astro-ph/0406297. doi:10.1111/j.1365-2966.2004.08120.x
Ricotti, M., Pontzen, A., Viel, M.: ApJL **663**, 53 (2007). 0706.0856. doi:10.1086/520113
Romano-Díaz, E., Shlosman, I., Hoffman, Y., Heller, C.: ApJL **685**, 105 (2008). 0808.0195. doi:10.1086/592687
Romano-Díaz, E., Shlosman, I., Heller, C., Hoffman, Y.: ApJ **702**, 1250 (2009). 0901.1317. doi:10.1088/0004-637X/702/2/1250
Ryden, B.S.: ApJ **329**, 589 (1988). doi:10.1086/166406
Ryden, B.S., Gunn, J.E.: ApJ **318**, 15 (1987). doi:10.1086/165349
Sand, D.J., Treu, T., Ellis, R.S.: ApJL **574**, 129 (2002). astro-ph/0207048. doi:10.1086/342530
Sand, D.J., Treu, T., Smith, G.P., Ellis, R.S.: ApJ **604**, 88 (2004). astro-ph/0309465. doi:10.1086/382146
Sawala, T., Frenk, C.S., Fattahi, A., Navarro, J.F., Theuns, T., Bower, R.G., Crain, R.A., Furlong, M., Jenkins, A., Schaller, M., Schaye, J.: ArXiv e-prints, 1406.6362 (2014). 1406.6362
Scoville, N.Z.: In: Falcón-Barroso, J., Knapen, J.H. (eds.) Evolution of star formation and gas, p. 491 (2013)
Shen, S., Wadsley, J., Stinson, G.: MNRAS **407**, 1581 (2010). 0910.5956. doi:10.1111/j.1365-2966.2010.17047.x
Simon, J.D., Bolatto, A.D., Leroy, A., Blitz, L.: ApJ **596**, 957 (2003). astro-ph/0307154. doi:10.1086/378200
Simon, J.D., Bolatto, A.D., Leroy, A., Blitz, L., Gates, E.L.: ApJ **621**, 757 (2005). astro-ph/0412035. doi:10.1086/427684
Sommer-Larsen, J., Dolgov, A.: ApJ **551**, 608 (2001). astro-ph/9912166. doi:10.1086/320211
Spano, M., Marcelin, M., Amram, P., Carignan, C., Epinat, B., Hernandez, O.: MNRAS **383**, 297 (2008). 0710.1345. doi:10.1111/j.1365-2966.2007.12545.x
Spedicato, E., Bodon, E., Del Popolo, A., Mahdavi-Amiri, N.: 4OR 1, 51 (2003). astro-ph/0209241. doi:10.1007/s10288-002-0004-0
Spitzer, L. Jr., Schwarzschild, M.: ApJ **114**, 385 (1951). doi:10.1086/145478
Stadel, J., Potter, D., Moore, B., Diemand, J., Madau, P., Zemp, M., Kuhlen, M., Quilis, V.: MNRAS **398**, 21 (2009). 0808.2981. doi:10.1111/j.1745-3933.2009.00699.x
Starobinsky, A.A.: Physics Letters B **91**, 99 (1980). doi:10.1016/0370-2693(80)90670-X
Stinson, G.S., Brook, C., Macciò, A.V., Wadsley, J., Quinn, T.R., Couchman, H.M.P.: MNRAS **428**, 129 (2013). 1208.0002. doi:10.1093/mnras/sts028
Stinson, G., Seth, A., Katz, N., Wadsley, J., Governato, F., Quinn, T.: MNRAS **373**, 1074 (2006). astro-ph/0602350. doi:10.1111/j.1365-2966.2006.11097.x
Strigari, L.E., Bullock, J.S., Kaplinghat, M.: ApJL **657**, 1 (2007). astro-ph/0701581. doi:10.1086/512976
Strigari, L.E., Frenk, C.S., White, S.D.M.: ArXiv e-prints, 1406.6079 (2014). 1406.6079
Swaters, R.A., Madore, B.F., van den Bosch, F.C., Balcells, M.: ApJ **583**, 732 (2003). astro-ph/0210152. doi:10.1086/345426
Takada, M.: In: Kawai, N., Nagataki, S. (eds.) American Institute of Physics Conference Series. American Institute of Physics Conference Series, vol. 1279, p. 120 (2010). doi:10.1063/1.3509247
Teyssier, R., Pontzen, A., Dubois, Y., Read, J.I.: MNRAS **429**, 3068 (2013). 1206.4895. doi:10.1093/mnras/sts563
Trujillo-Gomez, S., Klypin, A., Colín, P., Ceverino, D., Arraki, K.S., Primack, J.: MNRAS **446**, 1140 (2015). 1311.2910. doi:10.1093/mnras/stu2037
Utrobin, V.P., Chugai, N.N.: A&A **532**, 100 (2011). 1107.2145. doi:10.1051/0004-6361/201117137
van den Bergh, S., Abraham, R.G., Ellis, R.S., Tanvir, N.R., Santiago, B.X., Glazebrook, K.G.: AJ **112**, 359 (1996). astro-ph/9604161. doi:10.1086/118020
Wadsley, J.W., Stadel, J., Quinn, T.: New Astronomy **9**, 137 (2004). astro-ph/0303521. doi:10.1016/j.newast.2003.08.004

Walker, M.G., Peñarrubia, J.: ApJ **742**, 20 (2011). 1108.2404. doi:10.1088/0004-637X/742/1/20
Walter, F., Brinks, E., de Blok, W.J.G., Bigiel, F., Kennicutt, R.C. Jr., Thornley, M.D., Leroy, A.: AJ **136**, 2563 (2008). 0810.2125. doi:10.1088/0004-6256/136/6/2563
Weinberg, S.: Reviews of Modern Physics **61**, 1 (1989). doi:10.1103/RevModPhys.61.1
White, S.D.M.: ApJ **286**, 38 (1984). doi:10.1086/162573
White, S.D.M., Frenk, C.S.: ApJ **379**, 52 (1991). doi:10.1086/170483
Williams, L.L.R., Babul, A., Dalcanton, J.J.: ApJ **604**, 18 (2004). arXiv:astro-ph/0312002. doi:10.1086/381722
Wolf, J., Bullock, J.S.: ArXiv e-prints, 1203.4240 (2012). 1203.4240
Zentner, A.R., Bullock, J.S.: ApJ **598**, 49 (2003). astro-ph/0304292. doi:10.1086/378797
Zhao, H.: MNRAS **278**, 488 (1996). astro-ph/9509122
Zheng, R., Huang, Q.-G.: JCAP **3**, 2 (2011). 1010.3512. doi:10.1088/1475-7516/2011/03/002
Zolotov, A., Brooks, A.M., Willman, B., Governato, F., Pontzen, A., Christensen, C., Dekel, A., Quinn, T., Shen, S., Wadsley, J.: ApJ **761**, 71 (2012). 1207.0007. doi:10.1088/0004-637X/761/1/71

This manuscript was prepared with the AAS LaTeX macros v5.2.